Title: **Transcriptome landscape of a thermal-tolerant coral endosymbiont reveals molecular signatures of symbiosis and dysbiosis**

Anthony J. Bellantuono[a], Katherine E. Dougan[a], Camila Granados-Cifuentes[a,b], and Mauricio Rodriguez-Lanetty[a]

[a]Department of Biological Sciences, Florida International University, Miami, FL 33199; [b]Baruch College—The City University of New York, New York, NY 10010

Corresponding Author: Mauricio Rodriguez-Lanetty (rodmauri@fiu.edu)

Keywords: coral bleaching, *Symbiodinium*, *Aiptasia*, symbiosis, dysbiosis, transcriptomics, thermal tolerance

Abstract

Warming oceans disrupt the critical endosymbiosis between corals and their photosynthetic dinoflagellate endosymbionts of the family Symbiodiniaceae. *Durusdinium trenchii* is a heat-tolerant species of Symbiodiniaceae and enhances survival of its coral host, but the basis for tolerance is largely unknown. To identify the underpinnings of heat tolerance and symbiosis, we compared the *in hospite* and free-living transcriptomes of *D. trenchii* under stable temperature conditions and acute hyperthermal stress. We discovered that under stable conditions, *in hospite* cells exhibit lower transcriptional activity than free-living counterparts, suggesting the shutdown of genes uniquely required for a free-living lifestyle. However, under hyperthermal stress the transcriptional response was larger *in hospite*, indicating an exacerbated stress environment within the host cell. Significantly, we unraveled the molecular signatures of symbiont heat tolerance within the host, which is a critical step to enable the development of engineered endosymbionts as a tool for restoration of coral reefs.

Introduction

Reef-building corals engage in an obligate endosymbiosis with a diverse group of dinoflagellate algae in the family Symbiodiniaceae, which is composed of seven recently described genera (LaJeunesse et al., 2018). In this nutritional symbiosis, the algal partner transfers up to 90% of the carbon it fixes to the coral host (Muscatine et al., 1984). However, this critical mutualism is sensitive to environmental stressors and can break down in a process termed coral bleaching (Glynn, 1993), most commonly due to elevated seawater temperature linked to anthropogenic climate change (Hoegh-Guldberg, 1999). High temperature anomalies are continuing to intensify, with 2015–2016 exhibiting the most intense global bleaching event on record (Eakin et al., 2016; Hughes et al., 2017). Recent models forecast that mass bleaching will be an annual event before 2050 (Maynard et al., 2017). Even if dramatic international actions manage to limit warming to 1.5 °C, coral populations are predicted to remain in peril (Anthony et al., 2017).

There is an existing body of work demonstrating that the shift of the dominant symbiont (shuffling) or acquisition of new species of symbionts (switching) from the environment enables holobionts, the coral host and its diverse assemblage of symbionts, to better withstand climate-related increases in seawater temperatures (Baker, 2001; Berkelmans and Van Oppen, 2006; Jones et al., 2008; Rowan, 2004; Stat et al., 2006). More recently, significant differences in heat tolerance have been reported both within a single Symbiodiniaceae genus (Díaz-Almeyda et al., 2017) as well as between genera (Grégoire et al., 2017), revealing that different Symbiodiniaceae species have differing thermal optima and tolerances. A well-studied case is

57 *Durusdinium trenchii* (previously *Symbiodinium trenchii* [LaJeunesse et al., 2018]), an
58 ITS2 – D1a subtype within Clade D that has been shown to confer increases in heat
59 tolerance of between 1-1.5 °C to coral hosts (Berkelmans and Van Oppen, 2006;
60 Rowan, 2004). This heat tolerance is also observed in culture conditions; *D. trenchii* can
61 maintain maximum photosynthetic rates at elevated temperatures in comparison to the
62 majority of other investigated Symbiodiniaceae species (Grégoire et al., 2017).
63 However, alternate heat-resistant assemblages of host and symbiont come with a cost,
64 showing decreases in growth rates (Jones and Berkelmans, 2011; Little et al., 2004).
65 The potential benefits to corals hosting *D. trenchii* in response to increasingly
66 warm ocean conditions is not only evident in Pacific reef corals (Baker, 2003), where
67 this species of symbiont is genetically diverse and is thought to have originated, but
68 also in the Caribbean Sea, where it is thought to have invaded in the past half century
69 (Pettay et al., 2015). Silverstein et al. (Silverstein et al., 2017) have demonstrated that
70 the Caribbean scleractinian coral *Montastraea cavernosa* colonized by *D. trenchii*
71 persist *in hospite* on thermally stressed reefs, whereas conspecific corals hosting type
72 C3 symbionts underwent massive bleaching.
73 Due to the current ecological crisis facing corals, there has been a growing
74 movement to develop purposeful interventions to increase the thermal tolerance of
75 many heat-sensitive coral holobionts, including experimental evolution and interspecific
76 hybridizations (Chakravarti et al., 2017; Chan et al., 2018). Recently, the use of genome
77 editing approaches has been proposed, with the primary goal of engineering heat-
78 sensitive endosymbionts in order to produce more heat-tolerant coral holobionts (Levin
79 et al., 2017). This requires the characterization of molecular mechanisms used by heat-

80 resistant Symbiodiniaceae species so that taxa exhibiting less resistant phenotypes can
81 be genetically engineered into heat-resistant symbionts.
82 By using a transcriptomic approach, we aimed to characterize the mRNA profiles
83 associated with the response to thermal stress in the heat-resistant *D. trenchii*. We
84 assessed the gene expression response of the symbiont both in the free-living state and
85 *in hospite* when stably associated with a cnidarian host. This design allowed us to
86 gauge the effect of symbiosis on the molecular response of the symbiont to heat stress.
87 In order to achieve sufficient sequencing depth of *in hospite D. trenchii*, we implemented
88 a novel symbiont mRNA enrichment technique. This powerful comparative approach
89 also facilitated an examination of the molecular changes underlying the transition from a
90 free-living to symbiotic state. This represents the first work to characterize the
91 transcriptional modifications associated with *in hospite* and free-living states of a
92 Symbiodiniaceae, and the first to characterize the divergent stress responses between
93 the symbiotic and free-living environment in a very ecologically important coral
94 symbiont, *D. trenchii*.
95 Our investigation reveals the dramatic differences in gene expression between
96 symbiotic and free-living *D. trenchii*. Further, we show that these differences are
97 magnified under conditions of thermal stress. When *D. trenchii* are in symbiosis, we
98 note a significant downregulation of transcripts. This molecular signature suggests that
99 the host provides a stabilized environment for *D. trenchii* in contrast to the free-living
100 state. Under thermal stress, the more active transcriptomic response of the
101 dinoflagellate *in hospite* in comparison to the free-living state suggests that the
102 dinoflagellates are responding to a less hospitable cellular environment. This result

103 brings critical attention to the necessity of examining thermal stress responses of coral
104 endosymbionts *in hospite* in order to capture the molecular signature of coral holobiont
105 persistence. Studies based solely on free-living cultures provide a biased perspective
106 that is confounded by responses to an external environment markedly different from the
107 holobiont.
108

109 # Results and Discussion

110 **Transcriptome Analysis**

111 A reference transcriptome of 82,273 transcripts was assembled, filtered for non-
112 Symbiodiniaceae transcripts, and used as the basis for differential expression analysis
113 (NCBI TSA BioProject PRJNA508937). Principal component analysis (PCA) of all
114 analyzed transcripts shows dramatic separation of treatments by both symbiotic state as
115 well as thermal stress (Fig. 2*A*). PC1, the principal component separating *in hospite* and
116 free-living treatments, is driven by 11,933 transcripts and explains 40.5% of the
117 variance, whereas PC2, the axis separating thermal treatment, is driven by 11,904
118 transcripts and explains 15.5% of the variance.

119 Statistical analysis for the identification of differentially expressed transcripts
120 (FDR corrected p-value < 0.01, greater than $\log_2$ 2-fold difference) reveals that the *in*
121 *hospite* condition in *D. trenchii* is marked by a substantial downregulation of gene
122 expression, with 368 transcripts upregulated versus 1625 downregulated at the 28°C
123 (Fig. 3A). This larger level of downregulation *in hospite* is maintained under the heat
124 stress comparison (34°C), with 2799 transcripts downregulated versus 793 upregulated
125 in comparison to the free-living state (Fig. 3A). Notably, the *in hospite* response to heat

126 stress is much more pronounced than that in the free-living condition, with a total of 709
127 transcripts differentially regulated as a function of thermal stress *in hospite* versus 353
128 transcripts in the free-living condition (Fig. 3B). Out of the 709 transcripts involved in
129 the *in hospite* response to heat, 624 transcripts (365 upregulated and 259
130 downregulated) were specific to the *in hospite* condition as these transcripts were not
131 differentially expressed in response to thermal challenge in free-living *D. trenchii* (Fig.
132 3B). The transcriptional response to thermal stress shared between free-living and *in*
133 *hospite D. trenchii* represented only 12% of the heat-modulated transcriptional response
134 *in hospite* (Fig. 4). This shared response could be considered the core heat response,
135 with activity regardless of the symbiotic state of the algal endosymbiont. However, this
136 represents a minority of detected transcriptional activity. The majority of transcripts
137 involved in response to heat stress depend upon the symbiotic condition of the
138 dinoflagellate (e.g. whether the cell is *in hospite* or free-living). Our findings demonstrate
139 that *D. trenchii* has distinct transcriptomic profiles *in hospite* and in free-living states,
140 and further, that the transcriptomic heat stress response is vastly different between *in*
141 *hospite* and free-living conditions. This brings critical attention to the importance of
142 examining the response of Symbiodiniaceae holistically, as the responses in culture
143 may not be representative of *in hospite* endosymbionts. To date, the vast majority of
144 transcriptomic assessments of Symbiodiniaceae within the context of thermal stress
145 have been performed exclusively on free-living cultures (Barshis et al., 2014;
146 Baumgarten et al., 2013; Díaz-Almeyda et al., 2017; Gierz et al., 2017; Levin et al.,
147 2016; Rachel Ashley Levin et al., 2017; Liew et al., 2017; Xiang et al., 2015), and while
148 they have been insightful, they may present a reduced transcriptional picture of the

149 alterations that occur in Symbiodiniaceae *in hospite*. Only one other investigation
150 directly compared gene expression *in hospite* to free-living conditions (Rosic et al.,
151 2010), but it focused on only two heat-shock protein genes. We propose that it is
152 imperative to consider the *in hospite* environment in the assessment of
153 Symbiodiniaceae response to thermal stress, and that culture-based studies require
154 careful consideration when extending findings to *in hospite* conditions.

155 **A Small Core Thermal Stress Response is Shared Between Free-living and *in***
156 ***hospite D. trenchii***
157
158 Within the conserved transcriptional changes under thermal stress shared
159 between the free-living and *in hospite* states of *D. trenchii* (Fig. 3, Fig. 4), 57 transcripts
160 were upregulated and 28 downregulated. Examination at the transcript level reveals that
161 the magnitude of expression within these core transcripts is, overall, higher in free-living
162 *D. trenchii* than *in hospite* (Fig. 4). With a relatively small number of transcripts
163 representing the core response, we were not able to perform meaningful GO term
164 enrichment analysis. Instead, our interpretation of this small conserved core response is
165 based upon transcript annotations.
166 Though the core set of transcripts differentially expressed in response to thermal
167 stress (Fig. 3) represents the minority of transcriptional alterations under stress *in*
168 *hospite* and in free-living cells, it sheds light on key processes conserved in the *D.*
169 *trenchii* stress response independent of symbiotic state. These processes include
170 modifications to membrane fluidity, DNA repair, anion channel activity, spermidine
171 synthase upregulation, and transposition. With their indispensability in both the *in*
172 *hospite* and free-living stress responses, these associated transcripts are potentially

173 important candidates in the identification of the genetic basis for thermal tolerance in *D.*
174 *trenchii*.
175 Maintenance of membrane viscosity is critical for cell homeostasis as
176 hyperthermal stress increases the fluidity of membranes, potentially leading to
177 disintegration of the lipid bilayer (Allakhverdiev et al., 2008). In Symbiodiniaceae,
178 thylakoid membrane lipid composition is a key determinant of thermal-stress sensitivity
179 (Tchernov et al., 2004). Within the core heat stress response, we identify an ortholog to
180 a *fatty acyl-CoA desaturase*, an enzyme involved in the remodeling of cell membranes
181 for homeoviscous adaptation (Hazel, 1995) that is potentially critical in modifying fluidity
182 to accommodate increasing temperatures.
183 The upregulation of *apurinic endonuclease-redox protein* (*ARP*) both *in hospite*
184 and in free-living conditions suggests that repair to oxidative DNA base damage occur
185 in both conditions. The apurinic/apyrimidinic (AP) endonucleases are important DNA
186 repair enzymes involved in two overlapping pathways: DNA glycosylase-initiated base
187 excision and AP endonuclease-initiated nucleotide incision repair (Akishev et al., 2016).
188 In the context of heat stress, this may allow *D. trenchii* a faster response to DNA
189 damage than other Symbiodiniaceae species.
190 Anion channels, spermidine synthase, and retrotransposons are disparate
191 entities which can each serve as heat stress response mediators with many
192 downstream effectors. In plants, anion channels are a master regulator of stress
193 response (reviewed by Rob et al., 2012). In the core heat stress response, we find the
194 upregulation of a transcript putatively coding for aluminum-activated malate transporter
195 9 (ALMT9). In plants, ALMT9 is involved in the release of chloride currents in guard

196 cells and malate homoeostasis. In response to stress, the release of chloride and
197 malate leads to the rapid stomatal closure (Dreyer et al., 2012). Though the precise role
198 of ALMT9 in stress response in Symbiodiniaceae species is unknown, it may be
199 involved in downstream stress response signaling. A transcript coding for spermidine
200 synthase is also upregulated across heat stress treatments. Spermidine synthase in
201 *Arabidopsis* dramatically improves stress tolerance when overexpressed via its effect on
202 multiple downstream targets (Kasukabe et al., 2004), while exogenous application of the
203 protein increases antioxidant tolerance in creeping bentgrass (Li et al., 2015). An
204 additional transcript of the core response potentially acting as an upstream effector of
205 numerous targets codes for LINE-1 reverse transcriptase. Recent work by Chen et al.
206 (2018) identified Ty1-copia-type LTR retrotransposons in *Symbiodinium microadriaticum*
207 which are activated by heat stress, suggesting that this may be a mechanism for the
208 generation of genetic variation under heat stress. Diatoms also possess stress-activated
209 retrotransposons, which are postulated to serves as generators of genetic variability
210 (Maumus et al., 2009). The involvement of retrotransposons in stress response has also
211 been observed across taxa. In plants, retrotransposons are activated by stress and go
212 on to activate numerous host regulatory pathways (Grandbastien, 2015, 1998).

213 ***D. trenchii* response to heat stress depends on the symbiotic state**
214
215 The majority (88% *in hospite* and 76% free-living) of the transcriptional response
216 to thermal stress is specific to the symbiotic state of the dinoflagellate (Fig. 3B). Both
217 free-living and *in hospite D. trenchii* have distinct responses to a thermal challenge of
218 34°C not only at the level of transcript identity (Fig. 3), but also with regard to enriched
219 gene ontology terms which are unique to each symbiotic state (Fig. 5). *In hospite D.*

220 *trenchii* have transcriptional activity with parent GO terms such as mRNA transport, N-
221 terminal protein amino acid acetylation, and cellular response to temperature stimulus,
222 all of which are not enriched in the free-living transcriptomic response to heat stress
223 (Fig. 5). There is also a striking *in hospite*-specific decrease in GO terms within the
224 category "binding of sperm to zona pellucida" under heat stress. In the case of the free-
225 living state, negative regulation of viral genome replication is highly downregulated in
226 contrast to the symbiotic state (Fig. 5). While the analysis reveals that the majority of
227 ontologies affected by heat stress are disparate depending upon symbiotic state,
228 decreased activity of vesicle-mediated transport is a common theme in the heat stress
229 response of both *in hospite* and free-living *D. trenchii* (Fig. 5). Despite this particular
230 instance of overlap in function indicated by gene ontology analysis, the transcripts
231 underlying vesicle-mediated transport in free-living and symbiotic treatments are distinct
232 in the symbiotic and free-living conditions (Supplement_2_DEGs_Annotations.xlsx).
233 Remarkably, despite the more highly responsive transcriptome of *in hospite D.*
234 *trenchii* to heat stress than free-living cells, free-living *D. trenchii* mount a more dramatic
235 response to photoxidative stress than *in hospite* at both 28°C and 34°C (Fig. 6). Gene
236 ontology terms for thermoception and response to oxidative stress are also highly
237 represented in free-living *D. trenchii* at 34°C, whereas no enrichment is detected *in*
238 *hospite* (Fig. 6). This suggests that the intracellular environment of the host provides
239 some level of protection for the endosymbiont from some aspects of photothermal
240 stress, potentially by a modified light environment within the host. This is supported by
241 earlier work by Bhagooli and collaborators (Bhagooli et al., 2008), who found that
242 multiple genera of Symbiodiniaceae exposed to photothermal stress *in hospite* had

243 unaffected photosynthetic output and less impact to maximum quantum yield in
244 comparison to cultured cells across genera. Coral hosts possess multiple mechanisms
245 for sheltering endosymbionts including photoprotective host chromoproteins (Dove et
246 al., 2001; Quick et al., 2018; Salih et al., 2000; Smith et al., 2013) and other host-
247 mediated modifications to the internal light environment, such as scattering by the coral
248 skeleton (Enríquez et al., 2005; Wangpraseurt et al., 2012). While this sheltering *in*
249 *hospite* may, on its surface, appear contradictory, we posit that the *in hospite* state has
250 a more complex transcriptional response to thermal stress overall, but that the host may
251 reduce light stress.

252 By examining ontologies from differentially expressed transcripts exclusively
253 associated with free-living and *in hospite* treatments, we found that the *in hospite* heat
254 stress response is highly enriched for mRNA transport and cellular response to
255 temperature stimulus (Fig. 5). We suggest that host sheltering of *in hospite* cells from
256 light may contribute to a symbiont's capacity to maintain some cellular functions which
257 may be heavily impacted in unsheltered free-living cells. This may result in the mounting
258 of a more effective transcriptional response to heat stress. Under acute thermal stress,
259 yeast block mRNA transport of transcripts uninvolved in the heat stress response
260 (Saavedra et al., 1996). If unsheltered free-living cells are under more severe stress,
261 experiencing the unfiltered brunt of light in combination with heat stress, mRNA
262 transport may be highly inhibited, as suggested by our analyses.

263 The *in hospite* state also exhibits a dramatic reduction in GO term enrichment
264 within the biological process binding of sperm to zona pellucida, a response not
265 observed in the free-living comparison (Fig. 5). One of the transcripts underlying this

266 enrichment (TRINITY_DN30024_c0_g1_i6) has high identity to *sperm surface protein*
267 *Sp17*, a protein possessed by sperm which binds the zona pellucida during mammalian
268 fertilization, critical for cell adhesion (O'rand et al., 1995; Richardson et al., 1994). The
269 expression of the putative *Sp17* ortholog may function in the mediation of normal
270 symbiosis, potentially involved in adhesion between the symbiont and host, while the
271 observed decrease in expression may be a part of dysbiosis.
272 Taken together, the intracellular environment experienced by *in hospite*
273 symbionts represents a complex set of interactions between the host, the external
274 environment, and the endosymbiont. The disparate transcriptomes of stress *in hospite*
275 and free-living likely result from a combination of protection from some aspects of stress
276 by the host, the complexity of an intracellular environment compared with that of a free-
277 living cell, and further, the transcriptional activity involved in the mediation of the
278 symbiosis, as discussed in sections that follow.
279 **Alterations required for the transition between free-living and symbiotic states**
280 Comparing the *in hospite* and free-living transcriptomes of *D. trenchii* provides a
281 window into the alterations necessary for symbiotic living. Several processes are
282 exclusively enriched *in hospite* under non-stress conditions at 28°C, in comparison to
283 the free-living state (28°C symbiotic vs. 28°C free-living) (Fig. 6). Late endosome to
284 vacuole transport and mRNA cis splicing via spliceosome are both highly enriched *in*
285 *hospite* along with response to prostaglandin F. The roles of increased lysosome activity
286 and enhanced cis splicing in symbiosis are unknown, but complexities in
287 Symbiodiniaceae mRNA splicing, including trans-splicing (Zhang et al., 2007) and non-
288 canonical intron splicing (Aranda et al., 2016; Lin, 2011; Mendez et al., 2015) are well-

289 documented. The enrichment of response to prostaglandin F is extremely curious as the
290 highest concentrations of prostaglandins are found in corals, where these compounds
291 are produced by the host (Valmsen et al., 2001; Weinheimer and Spraggins, 1969).
292 Hydrogen peroxide catabolism is enriched *in hospite* at both 28°C and 34°C in
293 comparison to the free-living state, with higher activity at 34°C. Increased scavenging of
294 hydrogen peroxide *in hospite* could potentially be adaptive and necessary for
295 maintaining stable symbiosis, as while the release of peroxide in the free-living state is
296 likely of minimal detriment, the release of this form of ROS *in hospite* is held to induce
297 an immune response on the part of the host (reviewed by Weis, 2008).
298 In addition to the aforementioned enrichment of photooxidative stress terms in
299 the free-living state under thermal challenge (34°C), the transcripts upregulated in the
300 free-living state at 28°C are also enriched for numerous terms associated with response
301 to photooxidative stress. While this is amongst the highest activity of parent GO terms in
302 the free-living condition at both thermal treatments, no increase in enrichment is found
303 in the *in hospite* condition at either 28°C or 34°C. Dipeptide transport as well as
304 heterochromatin organization are also highly enriched in the free-living condition at
305 28°C.

306 ***D. trenchii* exhibits transcriptome reduction *in hospite***

307 Genome reduction is a common phenomenon in obligate microbial
308 endosymbionts (Martínez-Cano et al., 2015; McCutcheon and Moran, 2012) which can
309 occur via multiple mechanisms. In obligate intracellular endosymbioses, there are some
310 common demographic conditions imposed upon the endosymbiont, namely relatively
311 small effective population size of endosymbionts, restriction to specific hosts, and

312 limited recombination between endosymbiont strains within the host (Martínez-Cano et
313 al., 2015). These conditions set the stage for genetic drift and loss of genes that are not
314 essential *in hospite*. However, this appears to not be the case in coral endosymbiosis,
315 given that all sequenced Symbiodiniaceae genomes are of approximately one gigabase
316 in size (Aranda et al., 2016; Lin et al., 2015; Liu et al., 2018; Shoguchi et al., 2013), nor
317 should it be expected, given that the coral endosymbiont must maintain the full
318 complement of genes for free-living persistence, as the majority of corals uptake their
319 endosymbionts from the free-living environment (Baird et al., 2009; Richmond and
320 Hunter, 1990). Further, Symbiodiniaceae have been found to exist in a free-living state
321 in numerous environments, including sediments and other benthic substrates, as
322 epiphytes, and in the water column (Granados-Cifuentes et al., 2015; Littman et al.,
323 2008; Takabayashi et al., 2012).

324 Despite this lack of genome reduction in Symbiodiniaceae, we identified a
325 significant downregulation of gene expression *in hospite* compared to free-living *D.*
326 *trenchii* at both temperatures. Free-living Symbiodiniaceae appear to require to a larger
327 transcriptional repertoire to persist in an extracellular environment, for functions
328 presumably including motility and coping with fluctuations experienced outside of the
329 confines of a host cell. This substantial downregulation of transcripts *in hospite* is
330 associated with enrichment of transcripts associated with heterochromatin organization
331 histone H3-K9 methylation (Fig. S2). The hypermethylated state of cultured, free-living
332 Symbiodinaceae was demonstrated by ten Lohuis and Miller (ten Lohuis and Miller,
333 1998), but comparisons to the *in hospite* condition have not been performed. Our results
334 suggest that chromatin remodeling may play an important role in the switch between the

335 free-living state and endosymbiosis, contributing to the substantial downregulation
336 associated with the symbiotic life phase. We consider this resulting transcriptome
337 reduction analogous to the genome reduction observed in numerous obligate symbiotic
338 systems.

339 **The potential for sex in free-living Symbiodiniaceae**

340 In many species, sex and reproduction are inextricably linked, but for some, sex
341 represents a special occasion. For instance, consider a member of a taxon sister to the
342 dinoflagellates, the apicomplexan *Plasmodium falciparum*. This malaria-causing
343 parasite only engages in sexual reproduction within its mosquito host (Kooij and
344 Matuschewski, 2007; Talman et al., 2004). Be it frequent or rare, the function of sex,
345 despite its apparent ubiquity, is not a settled case. One hypothesis regarding the
346 evolution of sex is that recombination mediated by sexual reproduction arose as a
347 mechanism to repair DNA damage in an individual (Bernstein et al., 1985). A competing
348 hypothesis holds that the advantage of meiotic recombination resides in the genetic
349 diversity afforded to offspring (Burt, 2000; Otto, 2009).

350 The role of sexual reproduction in the Symbiodiniaceae life cycle remains an
351 open question. A broad survey of Symbiodiniaceae by Santos and Coffroth (2003)
352 concluded that Symbiodiniaceae are diploid in the vegetative life phase, both in cultured
353 and *in hospite* cells. However, apparent tetrads have long been reported in cultured
354 Symbiodiniaceae (Freudenthal, 1962), but it remains unknown whether these tetrad-like
355 arrangements represent meiotic events or simply two rounds of mitosis.
356 Symbiodiniaceae meiosis has yet to be demonstrated in an experimental setting, but
357 others have identified population genetic evidence of recombination (Baillie et al., 2000;

358 LaJeunesse, 2001). Further, Symbiodinaceae genomes possess a virtually complete
359 gene set for meiosis (Liu et al., 2018), suggesting that they have the potential for sexual
360 reproduction.

361 We posit that the free-living phase of life in Symbiodinacaea may provide the
362 opportunity for sex and recombination in the free-living state. In comparisons at 28°C,
363 several meiosis-related transcripts are upregulated in the free-living state in comparison
364 to the *in hospite* condition (*MSH6, RAD54*, *MEI2-like 2*, *MEI2-like 3*, and *MEI2-like 5*).
365 Our work also identifies a subset of these meiotic transcripts (three *MEI2-like 5*
366 transcripts*)* in the core heat stress response of *D. trenchii* that is shared by both *in*
367 *hospite* and free-living states. While Levin et al. (2016) also detected an upregulation of
368 meiosis-related genes under conditions of thermal stress in culture conditions, our work
369 adds a nuanced understanding of alterations in meiosis-related gene expression
370 between free-living and *in hospite D. trenchii*.

371 Recombination through sexual reproduction may be critical to the maintenance of
372 Symbiodiniaceae genomes. Muller's Ratchet dictates that asexual reproduction without
373 other forms of recombination has the potential for the accumulation of deleterious
374 mutations over generations (Felsenstein, 1974; Muller, 1964, 1932). This effect has
375 support from RNA viruses lacking recombination (Chao, 1997) and may be one of the
376 driving forces behind genome reduction in obligate endosymbionts (Andersson and
377 Kurland, 1998), but obligate symbionts may have other mechanisms to avert genomic
378 meltdown. Selection at the level of the holobiont has been suggested as one
379 mechanism of endosymbiont genome maintenance (Rispe and Moran, 2000), with
380 genomic degradation and losses observed likely to be neutral or nearly neutral

381 (Pettersson and Berg, 2007). We posit that recombination in the free-living phase of
382 Symbiodiniaceae may be instrumental in genomic maintenance of functions necessary
383 for the free-living state.

384 **Evasion of host immunity by symbiont-derived factors**

385 In order to maintain a stable endosymbiotic existence, members of the family
386 Symbiodiniaceae must evade the host immune system. A considerable number of
387 studies have shown that Symbiodiniaceae suppress and/or circumvent host immunity in
388 order to colonize and persist *in hospite*; multiple mechanisms of circumvention appear
389 to occur, including the suppression of apoptosis (Matthews et al., 2017; Rodriguez-
390 Lanetty et al., 2006; Tchernov et al., 2011) as well as the manipulation of markers of
391 endosome age (Chen et al., 2005, 2004, 2003). More recent work has identified
392 endosymbiont miRNAs which target host transcripts involved in immunity (Baumgarten
393 et al., 2018, 2013). We identified numerous transcripts involved in the suppression of
394 innate immunity and anti-inflammatory pathways, including a putative NRCL3 ortholog
395 and NF-κB inhibitor, which are upregulated in the symbiotic state. However, in order for
396 this to plausibly occur, the symbiont must be able transmit these signals to the host.
397 Based on transcriptome evidence, we postulate mechanisms for this below.

398 Apicomplexans, including parasites in the genus *Plasmodium,* possess
399 structures that form an apical complex which functions in host invasion and secretes
400 effectors into the host (reviewed by Kemp et al., 2013). Cellular machinery in
401 Symbiodinaceae involved in the delivery of immune-suppressing factors to the host
402 remain unexplored, but this work identifies several abundant transcripts with homology
403 to components of the apicomplexan apical complex. One component of the apical

404 complex are micronemes, bar-like organelles which release micronemal proteins critical
405 for host cell recognition and attachment, linking parasite and host cell receptors (Brecht
406 et al., 2001; Carruthers and Tomley, 2008; Friedrich et al., 2010; Soldati et al., 2001)
407 and further are critical for the trafficking and storage of ligands for host-cell receptors
408 (Soldati et al., 2001).

409 *D. trenchii* possess numerous transcripts with homology to proteins associated
410 with the apicomplexan apical complex, including three apical complex lysine
411 methyltransferase transcripts (TRINITY_DN22464_c0_g1_i2,
412 TRINITY_DN12687_c0_g1_i1, and TRINITY_DN59290_c0_g1_i1) and AGC/AKT
413 protein kinase transcripts (TRINITY_DN23213_c0_g1_i1 and
414 TRINITY_DN55685_c0_g1_i1), and three putative microneme proteins
415 (TRINITY_DN25568_c0_g1_i1, TRINITY_DN48019_c0_g1_i1, and
416 TRINITY_DN29950_c0_g1_i3). While the majority of these transcripts are not
417 differentially expressed, two are highly upregulated *in hospite*. One of these transcripts
418 (TRINITY_DN29950_c0_g1_i3) is a putative ortholog of a *Toxoplasma* microneme
419 protein 4 (MIC4). In its role in infection, the *Toxoplasma* MIC4 is thought to contribute to
420 parasite adhesion by acting as a bridge between receptors on the parasite and the host
421 cell (Brecht et al., 2001). Another transcript upregulated *in hospite* with homology to
422 apicomplexan invasion machinery is a cGMP-dependent protein kinase
423 (TRINITY_DN29950_c0_g1_i3) which Collins et al. (Collins et al., 2013) show is
424 required for the release of micronemes in *Plasmodium*. Taken together, these
425 transcripts suggest the possibility of components of an apicomplexan-like apical
426 complex involved in the maintenance of intracellular symbiosis by *D. trenchii*, and

427 potentially the delivery of symbiont-derived factors which suppress the host immune
428 response to allow stable endosymbiosis.

429 **Enhanced ammonium and ABC transporter activity *in hospite***

430 The controlled exchange of materials between the symbiont and host is of critical
431 importance for the persistence of both partners (Behie and Bidochka, 2014; Moya et al.,
432 2008). Our study identified transporters active in the symbiotic state for both ammonium
433 transport and assimilation, as well as a diverse group of ABC transporters which may be
434 involved in the movement of numerous as-yet unidentified substrates into and out the
435 symbiont.

436 The acquisition of inorganic nitrogen is of critical importance to photosynthetic
437 endosymbionts. Pernice et al. (2012) demonstrated that *in hospite* dinoflagellates fix 14
438 to 23 times more nitrogen than coral host cells in ammonium-enriched water. In the *in*
439 *hospite* state, we identify the upregulation of an ammonium transporter transcript as well
440 as two glutamine synthetase transcripts. This is congruent with the longstanding support
441 for glutamine synthetase activity as the mechanism by which Symbiodinacaea
442 assimilate ammonium from seawater and re-assimilate waste ammonium from the
443 cnidarian host (Anderson and Burris, 1987).

444 In the *in hospite* state, five transcripts annotated as ABC transporters are
445 upregulated in comparison to the free-living state at 28°C (Table S5). While numerous
446 host ABC transporters are upregulated in the proteomes of symbiotic *Exaiptasia pallida*
447 by Matthews et al. (2017), with earlier work by Peng et al. (2010) identifying an ABC
448 transporter associated with the symbiosome, this represents the first functional
449 evidence *in hospite* Symbiodiniaceae transporter activity in a cnidarian. ABC

450 transporters comprise a family of proteins responsible for the transport of diverse
451 substrates, including ions, nutrients, amino acids, peptides, proteins, lipids, metals,
452 lipids, oligonucleotides, and sugars (Locher, 2016; Wilkens, 2015).

453 **Conclusion**

454 In summary, our results demonstrate that symbiotic state has major impacts on
455 Symbiodiniaceae gene expression, both in steady state symbiosis and under conditions
456 of acute thermal stress. While prior work has found physiological differences between *in*
457 *hospite* and free-living Symbiodiniaceae (e.g. Banaszak and Trench, 1995; Bhagooli et
458 al., 2008), effect of the intracellular habitat on the transcriptome has not previously been
459 appreciated. The *in hospite* response to thermal stress differs dramatically from that of
460 free-living *D. trenchii*, with the transcriptome of *in hospite* endosymbionts hallmarked by
461 higher differential gene expression activity overall and enriched for mRNA transport
462 activity as well as a specialized cell adhesion process. While we identify a core heat
463 stress response shared between free-living and *in hospite D. trenchii*, this represents
464 only a minority of transcriptional activity. Our findings also reveal the distinct processes
465 at work in free-living and *in hospite* cells under non-stress conditions, with free-living *D.*
466 *trenchii* exhibiting evidence suggestive of sexual reproduction and *in hospite* cells
467 displaying reduced differential expression in a process we term transcriptome reduction,
468 as well as putative host evasion activity. We intend for this to serves as the basis for
469 future gene editing efforts to understand the genetic basis of symbiosis and dysbiosis,
470 with the ultimate aim of engineering of stress-tolerant coral endosymbionts. These
471 efforts will for provide additional options in future reef protection and restoration efforts
472 desperately needed for the persistence of coral reefs into the 21st century.

473

474 ## Materials and Methods

475 Aposymbiotic *Exaiptasia pallida* (strain CC7) were inoculated with *D. trenchii*
476 (strain CCMP2556) and maintained with feeding of *Artemia franciscana* twice weekly for
477 12 months. Free-living *D. trenchii* were cultured in Prov50 (Smith and Chanley, 1975)
478 medium and maintained in log phase via regular passage. To identify thermal
479 treatments that elicited an acute heat stress response, *Durusdinium trenchii* (strain
480 CCMP2556) cultures were exposed to thermal stress and assessed with PAM
481 fluorometry (Fig. S1). Based upon the observed rapid decline in Fv/Fm at 34 °C in
482 contrast to the maintained photosynthetic efficiency at 28 °C (Fig. S1), these treatments
483 were selected and implemented for comparisons following 6 hours at the target
484 temperatures. Symbiotic anemones and free-living *D. trenchii* cultures were held at
485 28°C under light intensity levels of 80 µE (12:12 light:dark cycle) and ramped up to the
486 34°C challenge at a rate of 2°C per day for thermal stress treatments, with increases of
487 temperature performed at the beginning of the photoperiod. Free-living (cultured) *D.*
488 *trenchii* and *in hospite D. trenchii* were frozen in liquid nitrogen mid-photoperiod for
489 sampling. Heat stress treatments were exposed to 34°C for a total of six hours. The
490 experiment was replicated temporally (n=3-4). Total RNA was extracted from
491 Symbiodiniaceae cells, with *in hospite* samples depleted of cnidarian host material prior
492 to extraction using a novel endosymbiont enrichment method (See Supplement 1 for
493 detailed methods). Stranded RNAseq libraries were prepared from poly(A) selected
494 RNA with the NEBNext Ultra RNA Library Prep Kit (NEB, Cambridge, MA) and
495 sequenced across two Illumina HiSeq lanes. A reference transcriptome was assembled

496 and filtered to remove host, other non-Symbiodiniaceae transcripts, and ribosomal RNA
497 transcripts. Principal component analysis was conducted using the prcomp function
498 from the stats package within R and statistical inference of significant transcripts driving
499 the principal components was conducting using the jackstraw package in R. The
500 resulting transcriptome was annotated using Trinotate (https://trinotate.github.io/) with
501 BLASTX and BLASTP searches performed against the SwissProt and Uniref90
502 databases using DIAMOND, an accelerated sequence aligner comparable to NCBI
503 BLAST+ (Buchfink et al., 2015). Following Trinotate, we employed the structural protein
504 homology detection program HH-Pred and the PDB70 database to identify remote
505 homologs in all remaining un-annotated transcripts using a strict cut-off of 80%
506 probability. Annotation was further supplemented by using Blast2GO (Conesa et al.,
507 2005) in combination with BLASTX searches against the non-redundant NCBI protein
508 database with DIAMOND and Interproscan under default settings. Gene ontology terms
509 acquired for each transcript during the annotation process from Trinotate, HHPred
510 (Söding et al., 2005), and Blast2GO were merged and redundant terms resulting from
511 the integration of the three annotation tools were removed prior to downstream
512 analyses. Following transcript quantification with Salmon (Patro et al., 2017), differential
513 gene expression analysis was performed in edgeR (Robinson et al., 2010) using a
514 generalized linear model to determine the effects of temperature and symbiotic state as
515 well as the interaction between the two on changes in transcript expression.
516 Differentially expressed transcripts were subject to gene ontology (GO) enrichment
517 analyses within the R package topGO (Alexa and Rahnenführer, 2016). GO results for

518 comparisons were visualized using REVIGO (Supek et al., 2011). Methods are
519 described in detail in Supplement 1.
520

521 ## Acknowledgements

522 We would like to thank Matthew DeGennaro and Ellen Dow for their input on final
523 stages of the manuscript. This research was funded by NSF-IOS CAREER (1453519)
524 and NSF-OCE RAPID (1503483) grants awarded to Mauricio Rodriguez-Lanetty.
525

526 ## References

527 Akishev Z, Taipakova S, Joldybayeva B, Zutterling C, Smekenov I, Ishchenko AA,
528 Zharkov DO, Bissenbaev AK, Saparbaev M. 2016. The major Arabidopsis thaliana
529 apurinic/apyrimidinic endonuclease, ARP is involved in the plant nucleotide incision
530 repair pathway. *DNA Repair (Amst)* **48**:30–42. doi:10.1016/j.dnarep.2016.10.009
531 Alexa A, Rahnenführer J. 2016. topGO: Enrichment Analysis for Gene Ontology. *R*
532 *Packag version 2320*.
533 Allakhverdiev SI, Kreslavski VD, Klimov V V., Los DA, Carpentier R, Mohanty P. 2008.
534 Heat stress: an overview of molecular responses in photosynthesis. *Photosynth*
535 *Res* **98**:541–550. doi:10.1007/s11120-008-9331-0
536 Anderson SL, Burris JE. 1987. Role of glutamine synthetase in ammonia assimilation by
537 symbiotic marine dinoflagellates (zooxanthellae). *Mar Biol* **94**:451–458.
538 doi:10.1007/BF00428252
539 Andersson SG., Kurland CG. 1998. Reductive evolution of resident genomes. *Trends*
540 *Microbiol* **6**:263–268. doi:10.1016/S0966-842X(98)01312-2

541 Anthony K, Bay LK, Costanza R, Firn J, Gunn J, Harrison P, Heyward A, Lundgren P,
542 Mead D, Moore T, Mumby PJ, van Oppen MJH, Robertson J, Runge MC, Suggett
543 DJ, Schaffelke B, Wachenfeld D, Walshe T. 2017. New interventions are needed to
544 save coral reefs. *Nat Ecol Evol* **1**:1420–1422. doi:10.1038/s41559-017-0313-5
545 Aranda M, Li Y, Liew YJ, Baumgarten S, Simakov O, Wilson MC, Piel J, Ashoor H,
546 Bougouffa S, Bajic VB, Ryu T, Ravasi T, Bayer T, Micklem G, Kim H, Bhak J,
547 LaJeunesse TC, Voolstra CR. 2016. Genomes of coral dinoflagellate symbionts
548 highlight evolutionary adaptations conducive to a symbiotic lifestyle. *Sci Rep*
549 **6**:39734. doi:10.1038/srep39734
550 Baillie BK, Baillie BK, Belda-baillie C a, Belda-baillie C a, Maruyama T, Maruyama T.
551 2000. Conspecificity and indo-pacific distribution of. *Analysis* **1161**:1153–1161.
552 Baird AH, Guest JR, Willis BL. 2009. Systematic and Biogeographical Patterns in the
553 Reproductive Biology of Scleractinian Corals. *Annu Rev Ecol Evol Syst* **40**:551–
554 571. doi:10.1146/annurev.ecolsys.110308.120220
555 Baker AC. 2003. Flexibility and Specificity in Coral-Algal Symbiosis: Diversity, Ecology,
556 and Biogeography of *Symbiodinium*. *Annu Rev Ecol Evol Syst* **34**:661–689.
557 doi:10.1146/annurev.ecolsys.34.011802.132417
558 Baker AC. 2001. Reef corals bleach to survive change. *Nature* **411**:765–766.
559 doi:10.1038/35081151
560 Banaszak AT, Trench RK. 1995. Effects of ultraviolet (UV) radiation on marine
561 microalgal-invertebrate symbioses .1. Response of the algal symbionts in culture
562 and in hospite. *J Exp Mar Bio Ecol* **194**:213–232. doi:Doi 10.1016/0022-
563 0981(95)00072-0

564 Barshis DJ, Ladner JT, Oliver TA, Palumbi SR. 2014. Lineage-Specific Transcriptional
565 Profiles of Symbiodinium spp. Unaltered by Heat Stress in a Coral Host. *Mol Biol*
566 *Evol* **31**:1343–1352. doi:10.1093/molbev/msu107
567 Baumgarten S, Bayer T, Aranda M, Liew YJ, Carr A, Micklem G, Voolstra CR. 2013.
568 Integrating microRNA and mRNA expression profiling in Symbiodinium
569 microadriaticum, a dinoflagellate symbiont of reef-building corals. *BMC Genomics*
570 **14**:704. doi:10.1186/1471-2164-14-704
571 Baumgarten S, Cziesielski MJ, Thomas L, Michell CT, Esherick LY, Pringle JR, Aranda
572 M, Voolstra CR. 2018. Evidence for miRNA-mediated modulation of the host
573 transcriptome in cnidarian–dinoflagellate symbiosis. *Mol Ecol* **27**:403–418.
574 doi:10.1111/mec.14452
575 Behie SW, Bidochka MJ. 2014. Nutrient transfer in plant-fungal symbioses. *Trends*
576 *Plant Sci*. doi:10.1016/j.tplants.2014.06.007
577 Berkelmans R, Van Oppen MJH. 2006. The role of zooxanthellae in the thermal
578 tolerance of corals: A “nugget of hope” for coral reefs in an era of climate change.
579 *Proc R Soc B Biol Sci* **273**:2305–2312. doi:10.1098/rspb.2006.3567
580 Bernstein H, Byerly H, Hopf F, Michod R. 1985. Genetic damage, mutation, and the
581 evolution of sex. *Science (80-)* **229**:1277–1281.
582 Bhagooli R, Baird AH, Ralph PJ. 2008. Does the coral host protect its algal symbionts
583 from heat and light stresses?Proceedings of the 11th International Coral Reef
584 Symposium. pp. 7–11.
585 Bolger AM, Lohse M, Usadel B. 2014. Trimmomatic: a flexible trimmer for Illumina
586 sequence data. *Bioinformatics* **30**:2114–20. doi:10.1093/bioinformatics/btu170

587 Brecht S, Carruthers VB, Ferguson DJ, Giddings OK, Wang G, Jakle U, Harper JM,
588 Sibley LD, Soldati D. 2001. The toxoplasma micronemal protein MIC4 is an adhesin
589 composed of six conserved apple domains. *J Biol Chem* **276**:4119–27.
590 doi:10.1074/jbc.M008294200
591 Buchfink B, Xie C, Huson DH. 2015. Fast and sensitive protein alignment using
592 DIAMOND. *Nat Methods* **12**:59–60. doi:10.1038/nmeth.3176
593 Burt A. 2000. Perspective: sex, recombination, and the efficacy of selection—was
594 Weismann right? *Evolution (N Y)* **54**:337–351. doi:10.1111/j.0014-
595 3820.2000.tb00038.x
596 Carruthers VB, Tomley FM. 2008. Microneme Proteins in ApicomplexansMolecular
597 Mechanisms of Parasite Invasion. New York, NY: Springer New York. pp. 33–45.
598 doi:10.1007/978-0-387-78267-6_2
599 Chakravarti LJ, Beltran VH, van Oppen MJH. 2017. Rapid thermal adaptation in
600 photosymbionts of reef-building corals. *Glob Chang Biol* **23**:4675–4688.
601 doi:10.1111/gcb.13702
602 Chan WY, Peplow LM, Menéndez P, Hoffmann AA, van Oppen MJH. 2018. Interspecific
603 Hybridization May Provide Novel Opportunities for Coral Reef Restoration. *Front*
604 *Mar Sci* **5**:160. doi:10.3389/fmars.2018.00160
605 Chao L. 1997. Evolution of sex and the molecular clock in RNA viruses. *Gene*.
606 doi:10.1016/S0378-1119(97)00405-8
607 Chen JE, Cui G, Wang X, Liew YJ, Aranda M. 2018. Recent expansion of heat-
608 activated retrotransposons in the coral symbiont Symbiodinium microadriaticum.
609 *ISME J* **12**:639–643. doi:10.1038/ismej.2017.179

610 Chen M-C, Cheng Y-M, Hong M-C, Fang L-S. 2004. Molecular cloning of Rab5
611 (ApRab5) in Aiptasia pulchella and its retention in phagosomes harboring live
612 zooxanthellae. *Biochem Biophys Res Commun* **324**:1024–1033.
613 doi:10.1016/J.BBRC.2004.09.151
614 Chen M-C, Cheng Y-M, Sung P-J, Kuo C-E, Fang L-S. 2003. Molecular identification of
615 Rab7 (ApRab7) in Aiptasia pulchella and its exclusion from phagosomes harboring
616 zooxanthellae. *Biochem Biophys Res Commun* **308**:586–595. doi:10.1016/S0006-
617 291X(03)01428-1
618 Chen M-C, Hong M-C, Huang Y-S, Liu M-C, Cheng Y-M, Fang L-S. 2005. ApRab11, a
619 cnidarian homologue of the recycling regulatory protein Rab11, is involved in the
620 establishment and maintenance of the Aiptasia–Symbiodinium endosymbiosis.
621 *Biochem Biophys Res Commun* **338**:1607–1616. doi:10.1016/J.BBRC.2005.10.133
622 Collins CR, Hackett F, Strath M, Penzo M, Withers-Martinez C, Baker DA, Blackman
623 MJ. 2013. Malaria Parasite cGMP-dependent Protein Kinase Regulates Blood
624 Stage Merozoite Secretory Organelle Discharge and Egress. *PLoS Pathog*
625 **9**:e1003344. doi:10.1371/journal.ppat.1003344
626 Conesa A, Götz S, García-Gómez JM, Terol J, Talón M, Robles M. 2005. Blast2GO: a
627 universal tool for annotation, visualization and analysis in functional genomics
628 research. *Bioinformatics* **21**:3674–6. doi:10.1093/bioinformatics/bti610
629 Díaz-Almeyda EM, Prada C, Ohdera AH, Moran H, Civitello DJ, Iglesias-Prieto R, Carlo
630 TA, LaJeunesse TC, Medina M. 2017. Intraspecific and interspecific variation in
631 thermotolerance and photoacclimation in Symbiodinium dinoflagellates. *Proc R Soc*
632 *B Biol Sci* **284**:20171767. doi:10.1098/rspb.2017.1767

633 Dove SG, Hoegh-Guldberg O, Ranganathan S. 2001. Major colour patterns of reef-
634 building corals are due to a family of GFP-like proteins. *Coral Reefs* **19**:197–204.
635 doi:10.1007/PL00006956
636 Dreyer I, Lucia Gomez-Porras J, Riaño-Pachón DM, Hedrich R, Geiger D, Geisler M.
637 2012. Molecular evolution of slow and quick anion channels (SLACs and
638 QUACs/ALMTs). doi:10.3389/fpls.2012.00263
639 Eakin CM, Liu G, Gomez AM, De La Cour JL, Heron SF, Skirving WJ, Geiger EF, Tirak
640 K V., Strong Alan E. 2016. Global coral bleaching 2014–2017: status and an appeal
641 for observations. *Reef Encount* **31**:20–26.
642 Edgar RC. 2010. Search and clustering orders of magnitude faster than BLAST.
643 *Bioinformatics* **26**:2460–2461. doi:10.1093/bioinformatics/btq461
644 Enríquez S, Méndez ER, -Prieto RI. 2005. Multiple scattering on coral skeletons
645 enhances light absorption by symbiotic algae. *Limnol Oceanogr* **50**:1025–1032.
646 doi:10.4319/lo.2005.50.4.1025
647 Felsenstein J. 1974. The evolutionary advantage of recombination. *Genetics* **78**:737–
648 56.
649 Freudenthal H. 1962. *Symbiodinium* gen. nov. and Symbiodinium microadriaticum sp.
650 nov., a Zooxanthella: Taxonomy, Life Cycle, and Morphology. *J Protozool* **9**:45–52.
651 doi:10.1111/j.1550-7408.1962.tb02579.x
652 Friedrich N, Santos JM, Liu Y, Palma AS, Leon E, Saouros S, Kiso M, Blackman MJ,
653 Matthews S, Feizi T, Soldati-Favre D. 2010. Members of a novel protein family
654 containing microneme adhesive repeat domains act as sialic acid-binding lectins
655 during host cell invasion by apicomplexan parasites. *J Biol Chem* **285**:2064–2076.

656 doi:10.1074/jbc.M109.060988
657 Gierz SL, Forêt S, Leggat W. 2017. Transcriptomic Analysis of Thermally Stressed
658 <i>Symbiodinium<i/> Reveals Differential Expression of Stress and Metabolism
659 Genes. *Front Plant Sci* **8**:271. doi:10.3389/fpls.2017.00271
660 Glynn PW. 1993. Coral reef bleaching: ecological perspectives. *Coral Reefs* **12**:1–17.
661 doi:10.1007/BF00303779
662 Grabherr MG, Haas BJ, Yassour M, Levin JZ, Thompson DA, Amit I, Adiconis X, Fan L,
663 Raychowdhury R, Zeng Q, Chen Z, Mauceli E, Hacohen N, Gnirke A, Rhind N, di
664 Palma F, Birren BW, Nusbaum C, Lindblad-Toh K, Friedman N, Regev A. 2011.
665 Full-length transcriptome assembly from RNA-Seq data without a reference
666 genome. *Nat Biotechnol* **29**:644–652. doi:10.1038/nbt.1883
667 Granados-Cifuentes C, Neigel J, Leberg P, Rodriguez-Lanetty M. 2015. Genetic
668 diversity of free-living Symbiodinium in the Caribbean: the importance of habitats
669 and seasons. *Coral Reefs* **34**:927–939. doi:10.1007/s00338-015-1291-1
670 Grandbastien M-A. 2015. LTR retrotransposons, handy hitchhikers of plant regulation
671 and stress response. *Biochim Biophys Acta - Gene Regul Mech* **1849**:403–416.
672 doi:10.1016/j.bbagrm.2014.07.017
673 Grandbastien MA. 1998. Activation of plant retrotransposons under stress conditions.
674 *Trends Plant Sci*. doi:10.1016/S1360-1385(98)01232-1
675 Grégoire V, Schmacka F, Coffroth MA, Karsten U. 2017. Photophysiological and
676 thermal tolerance of various genotypes of the coral endosymbiont *Symbiodinium*
677 sp. (Dinophyceae). *J Appl Phycol* **29**:1893–1905. doi:10.1007/s10811-017-1127-1
678 Hazel JR. 1995. Thermal Adaptation in Biological Adaptation: Is Homeoviscous

679 Adaptation the Explanation?, AmlU. Rev. Physiol.
680 Hoegh-Guldberg O. 1999. Climate change, coral bleaching and the future of the world's
681 coral reefs. *Mar Freshw Res* **50**:839. doi:10.1071/MF99078
682 Hughes TP, Kerry JT, Álvarez-Noriega M, Álvarez-Romero JG, Anderson KD, Baird AH,
683 Babcock RC, Beger M, Bellwood DR, Berkelmans R, Bridge TC, Butler IR, Byrne
684 M, Cantin NE, Comeau S, Connolly SR, Cumming GS, Dalton SJ, Diaz-Pulido G,
685 Eakin CM, Figueira WF, Gilmour JP, Harrison HB, Heron SF, Hoey AS, Hobbs J-
686 PA, Hoogenboom MO, Kennedy E V., Kuo C, Lough JM, Lowe RJ, Liu G,
687 McCulloch MT, Malcolm HA, McWilliam MJ, Pandolfi JM, Pears RJ, Pratchett MS,
688 Schoepf V, Simpson T, Skirving WJ, Sommer B, Torda G, Wachenfeld DR, Willis
689 BL, Wilson SK. 2017. Global warming and recurrent mass bleaching of corals.
690 *Nature* **543**:373–377. doi:10.1038/nature21707
691 Jones AM, Berkelmans R. 2011. Tradeoffs to Thermal Acclimation: Energetics and
692 Reproduction of a Reef Coral with Heat Tolerant *Symbiodinium* Type-D. *J Mar Biol*
693 **2011**:1–12. doi:10.1155/2011/185890
694 Jones AM, Berkelmans R, van Oppen MJH, Mieog JC, Sinclair W. 2008. A community
695 change in the algal endosymbionts of a scleractinian coral following a natural
696 bleaching event: field evidence of acclimatization. *Proceedings Biol Sci* **275**:1359–
697 65. doi:10.1098/rspb.2008.0069
698 Kasukabe Y, He L, Nada K, Misawa S, Ihara I, Tachibana S. 2004. Overexpression of
699 Spermidine Synthase Enhances Tolerance to Multiple Environmental Stresses and
700 Up-Regulates the Expression of Various Stress-Regulated Genes in Transgenic
701 Arabidopsis thaliana, Plant Cell Physiol.

702 Kemp LE, Yamamoto M, Soldati-Favre D. 2013. Subversion of host cellular functions by
703 the apicomplexan parasites. *FEMS Microbiol Rev* **37**:607–631. doi:10.1111/1574-
704 6976.12013
705 Kim D, Langmead B, Salzberg SL. 2015. HISAT: a fast spliced aligner with low memory
706 requirements. *Nat Methods* **12**:357–360. doi:10.1038/nmeth.3317
707 Kooij TW, Matuschewski K. 2007. Triggers and tricks of Plasmodium sexual
708 development. *Curr Opin Microbiol* **10**:547–553. doi:10.1016/J.MIB.2007.09.015
709 LaJeunesse TC. 2001. Investigating the Biodiversity, Ecology, and Phylogeny of
710 Endosymbiotic Dinoflagellates in the Genus symbiodinium using the Its Region: In
711 Search of a “species” Level Marker. *J Phycol* **37**:866–880.
712 LaJeunesse TC, Parkinson JE, Gabrielson PW, Jeong HJ, Reimer JD, Voolstra CR,
713 Santos SR. 2018. Systematic Revision of Symbiodiniaceae Highlights the Antiquity
714 and Diversity of Coral Endosymbionts. *Curr Biol* **28**:2570–2580.e6.
715 doi:10.1016/J.CUB.2018.07.008
716 Langmead B, Salzberg SL. 2012. Fast gapped-read alignment with Bowtie 2. *Nat*
717 *Methods* **9**:357–359. doi:10.1038/nmeth.1923
718 Levin RA, Beltran VH, Hill R, Kjelleberg S, McDougald D, Steinberg PD, van Oppen
719 MJH. 2016. Sex, Scavengers, and Chaperones: Transcriptome Secrets of
720 Divergent *Symbiodinium* Thermal Tolerances. *Mol Biol Evol* **33**:2201–2215.
721 doi:10.1093/molbev/msw119
722 Levin RA, Voolstra CR, Agrawal S, Steinberg PD, Suggett DJ, van Oppen MJH. 2017.
723 Engineering Strategies to Decode and Enhance the Genomes of Coral Symbionts.
724 *Front Microbiol* **8**:1220. doi:10.3389/fmicb.2017.01220

725 Levin RA, Voolstra CR, Weynberg KD, van Oppen MJH. 2017. Evidence for a role of
726 viruses in the thermal sensitivity of coral photosymbionts. *ISME J* **11**:808–812.
727 doi:10.1038/ismej.2016.154
728 Li Z, Zhou H, Peng Y, Zhang X, Ma X, Huang L, Yan Y. 2015. Exogenously applied
729 spermidine improves drought tolerance in creeping bentgrass associated with
730 changes in antioxidant defense, endogenous polyamines and phytohormones.
731 *Plant Growth Regul* **76**:71–82. doi:10.1007/s10725-014-9978-9
732 Liew YJ, Li Y, Baumgarten S, Voolstra CR, Aranda M. 2017. Condition-specific RNA
733 editing in the coral symbiont Symbiodinium microadriaticum. *PLOS Genet*
734 **13**:e1006619. doi:10.1371/journal.pgen.1006619
735 Lin S. 2011. Genomic understanding of dinoflagellates. *Res Microbiol* **162**:551–569.
736 doi:10.1016/J.RESMIC.2011.04.006
737 Lin S, Cheng S, Song B, Zhong X, Lin X, Li W, Li L, Zhang Y, Zhang H, Ji Z, Cai M,
738 Zhuang Y, Shi X, Lin L, Wang L, Wang Z, Liu X, Yu S, Zeng P, Hao H, Zou Q,
739 Chen C, Li Y, Wang Y, Xu C, Meng S, Xu X, Wang J, Yang H, Campbell DA, Sturm
740 NR, Dagenais-Bellefeuille S, Morse D. 2015. The Symbiodinium kawagutii genome
741 illuminates dinoflagellate gene expression and coral symbiosis. *Science* **350**:691–4.
742 doi:10.1126/science.aad0408
743 Little AF, van Oppen MJH, Willis BL. 2004. Flexibility in Algal Endosymbioses Shapes
744 Growth in Reef Corals. *Science (80-)* **304**:1492–1495.
745 doi:10.1126/science.1095733
746 Littman RA, van Oppen MJH, Willis BL. 2008. Methods for sampling free-living
747 Symbiodinium (zooxanthellae) and their distribution and abundance at Lizard Island

748 (Great Barrier Reef). *J Exp Mar Bio Ecol* **364**:48–53.
749 doi:10.1016/J.JEMBE.2008.06.034
750 Liu H, Stephens TG, González-Pech RA, Beltran VH, Lapeyre B, Bongaerts P, Cooke I,
751 Aranda M, Bourne DG, Forêt S, Miller DJ, van Oppen MJH, Voolstra CR, Ragan
752 MA, Chan CX. 2018. Symbiodinium genomes reveal adaptive evolution of functions
753 related to coral-dinoflagellate symbiosis. *Commun Biol* **1**:95. doi:10.1038/s42003-
754 018-0098-3
755 Locher KP. 2016. Mechanistic diversity in ATP-binding cassette (ABC) transporters. *Nat*
756 *Struct Mol Biol* **23**:487–493. doi:10.1038/nsmb.3216
757 Martínez-Cano DJ, Reyes-Prieto M, Martínez-Romero E, Partida-Martínez LP, Latorre
758 A, Moya A, Delaye L. 2015. Evolution of small prokaryotic genomes. *Front*
759 *Microbiol* **6**:742. doi:10.3389/fmicb.2014.00742
760 Matthews JL, Crowder CM, Oakley CA, Lutz A, Roessner U, Meyer E, Grossman AR,
761 Weis VM, Davy SK. 2017. Optimal nutrient exchange and immune responses
762 operate in partner specificity in the cnidarian-dinoflagellate symbiosis. *Proc Natl*
763 *Acad Sci* **114**:201710733. doi:10.1073/pnas.1710733114
764 Maumus F, Allen AE, Mhiri C, Hu H, Jabbari K, Vardi A, Grandbastien M-A, Bowler C.
765 2009. Potential impact of stress activated retrotransposons on genome evolution in
766 a marine diatom. *BMC Genomics* **10**:624. doi:10.1186/1471-2164-10-624
767 Maynard J, Marshall P, Parker B, Mcleod E, Ahmadia G, van Hooidonk R, Planes S,
768 Williams G, Raymundo L, Beeden R, Tamelander J. 2017. Coral Bleaching
769 Futures. Nairobi. doi:10.1007/978-3-540-69775-6
770 McCutcheon JP, Moran NA. 2012. Extreme genome reduction in symbiotic bacteria. *Nat*

771 *Rev Microbiol*. doi:10.1038/nrmicro2670
772 Mendez GS, Delwiche CF, Apt KE, Lippmeier JC. 2015. Dinoflagellate Gene Structure
773 and Intron Splice Sites in a Genomic Tandem Array. *J Eukaryot Microbiol* **62**:679–
774 687. doi:10.1111/jeu.12230
775 Moya A, Peretó J, Gil R, Latorre A. 2008. Learning how to live together: Genomic
776 insights into prokaryote-animal symbioses. *Nat Rev Genet*. doi:10.1038/nrg2319
777 Muller HJ. 1964. The relation of recombination to mutational advance. *Mutat Res Mol*
778 *Mech Mutagen* **1**:2–9. doi:10.1016/0027-5107(64)90047-8
779 Muller HJ. 1932. Some Genetic Aspects of Sex. *Am Nat* **66**:118–138.
780 doi:10.1086/280418
781 Muscatine L, Falkowski PG, Porter JW, Dubinsky Z. 1984. Fate of Photosynthetic Fixed
782 Carbon in Light- and Shade-Adapted Colonies of the Symbiotic Coral Stylophora
783 pistillata. *Proc R Soc B Biol Sci* **222**:181–202. doi:10.1098/rspb.1984.0058
784 O'rand MG, Richardson RT, Yamasaki N. 1995. Expression of the rabbit sperm protein
785 Sp17 in cos cells and interaction of recombinant Sp17 with the rabbit zona
786 pellucida. *Mol Reprod Dev* **40**:48–55. doi:10.1002/mrd.1080400107
787 Otto SP. 2009. The Evolutionary Enigma of Sex. *Am Nat* **174**:S1–S14.
788 doi:10.1086/599084
789 Patro R, Duggal G, Love MI, Irizarry RA, Kingsford C. 2017. Salmon provides fast and
790 bias-aware quantification of transcript expression. *Nat Methods* **14**:417–419.
791 doi:10.1038/nmeth.4197
792 Peng S-E, Wang Y-B, Wang L-H, Chen W-NU, Lu C-Y, Fang L-S, Chen C-S. 2010.
793 Proteomic analysis of symbiosome membranes in Cnidaria-dinoflagellate

794 endosymbiosis. *Proteomics* **10**:NA-NA. doi:10.1002/pmic.200900595
795 Pernice M, Meibom A, Van Den Heuvel A, Kopp C, Domart-Coulon I, Hoegh-Guldberg
796 O, Dove S. 2012. A single-cell view of ammonium assimilation in coral-
797 dinoflagellate symbiosis Subject Category: microbe-microbe and microbe-host
798 interactions. *ISME J*. doi:10.1038/ismej.2011.196
799 Pettay DT, Wham DC, Smith RT, Iglesias-Prieto R, LaJeunesse TC. 2015. Microbial
800 invasion of the Caribbean by an Indo-Pacific coral zooxanthella. *Proc Natl Acad Sci*
801 **112**:7513–7518. doi:10.1073/pnas.1502283112
802 Pettersson ME, Berg OG. 2007. Muller's ratchet in symbiont populations. *Genetica*
803 **130**:199–211. doi:10.1007/s10709-006-9007-7
804 Quast C, Pruesse E, Yilmaz P, Gerken J, Schweer T, Yarza P, Peplies J, Glöckner FO.
805 2012. The SILVA ribosomal RNA gene database project: improved data processing
806 and web-based tools. *Nucleic Acids Res* **41**:D590–D596. doi:10.1093/nar/gks1219
807 Quick C, D'Angelo C, Wiedenmann J. 2018. Trade-Offs Associated with Photoprotective
808 Green Fluorescent Protein Expression as Potential Drivers of Balancing Selection
809 for Color Polymorphism in Reef Corals. *Front Mar Sci* **5**:11.
810 doi:10.3389/fmars.2018.00011
811 Richardson RT, Yamasaki N, O'rand MG. 1994. Sequence of arabbit sperm zona
812 pellucida binding protein and localization during the acrosome reaction. *Dev Biol*
813 **165**:688–701. doi:10.1006/dbio.1994.1285
814 Richmond RH, Hunter CL. 1990. Reproduction and recruitment of corals: comparisons
815 among the Caribbean, the Tropical Pacific, and the Red Sea*.
816 Rispe C, Moran NA. 2000. Accumulation of Deleterious Mutations in Endosymbionts:

817 Muller's Ratchet with Two Levels of Selection. *Am Nat* **156**:425–441.
818 doi:10.1086/303396
819 Rob M, Roelfsema G, Hedrich R, Geiger D. 2012. Anion channels: master switches of
820 stress responses. *Trends Plant Sci* **17**:221–229. doi:10.1016/j.tplants.2012.01.009
821 Robinson MD, McCarthy DJ, Smyth GK. 2010. edgeR: a Bioconductor package for
822 differential expression analysis of digital gene expression data. *Bioinformatics*
823 **26**:139–40. doi:10.1093/bioinformatics/btp616
824 Rodriguez-Lanetty M, Phillips W, Weis V. 2006. Transcriptome analysis of a cnidarian –
825 dinoflagellate mutualism reveals complex modulation of host gene expression.
826 *BMC Genomics* **7**:23. doi:10.1186/1471-2164-7-23
827 Rosic NN, Pernice M, Dunn S, Dove S, Hoegh-Guldberg O. 2010. Differential regulation
828 by heat stress of novel cytochrome P450 genes from the dinoflagellate symbionts
829 of reef-building corals. *Appl Environ Microbiol* **76**:2823–9. doi:10.1128/AEM.02984-
830 09
831 Rowan R. 2004. Thermal adaptation in reef coral symbionts. *Nature* **430**:742.
832 Saavedra C, Tuug KS, Amberg DC, Hopper AK, Cole CN. 1996. Regulation of mRNA
833 export in response to stress in Saccharomyces cerevisiae. *Genes Dev* **10**:1608–
834 1620. doi:10.1101/gad.10.13.1608
835 Salih A, Larkum A, Cox G, Kuhl M, Hoegh-Guldberg O. 2000. Fluorescent pigments in
836 corals are photoprotective. *Nature* **408**:850–853.
837 Santos SR, Coffroth MA. 2003. Molecular Genetic Evidence that Dinoflagellates
838 Belonging to the Genus Symbiodinium Freudenthal Are Haploid.
839 Shoguchi E, Shinzato C, Kawashima T, Gyoja F, Mungpakdee S, Koyanagi R, Takeuchi

840 T, Hisata K, Tanaka M, Fujiwara M, Hamada M, Seidi A, Fujie M, Usami T, Goto H,
841 Yamasaki S, Arakaki N, Suzuki Y, Sugano S, Toyoda A, Kuroki Y, Fujiyama A,
842 Medina M, Coffroth MA, Bhattacharya D, Satoh N. 2013. Draft Assembly of the
843 Symbiodinium minutum Nuclear Genome Reveals Dinoflagellate Gene Structure.
844 *Curr Biol* **23**:1399–1408. doi:10.1016/J.CUB.2013.05.062
845 Silverstein RN, Cunning R, Baker AC. 2017. Tenacious D: *Symbiodinium* in clade D
846 remain in reef corals at both high and low temperature extremes despite
847 impairment. *J Exp Biol* **220**:1192–1196. doi:10.1242/jeb.148239
848 Smith-Unna R, Boursnell C, Patro R, Hibberd JM, Kelly S. 2016. TransRate: reference-
849 free quality assessment of de novo transcriptome assemblies. *Genome Res*
850 **26**:1134–44. doi:10.1101/gr.196469.115
851 Smith EG, D'Angelo C, Salih A, Wiedenmann J. 2013. Screening by coral green
852 fluorescent protein (GFP)-like chromoproteins supports a role in photoprotection of
853 zooxanthellae. *Coral Reefs* **32**:463–474. doi:10.1007/s00338-012-0994-9
854 Smith WL, Chanley MH, editors. 1975. Culture of Marine Invertebrate Animals. Boston,
855 MA: Springer US. doi:10.1007/978-1-4615-8714-9
856 Söding J, Biegert A, Lupas AN. 2005. The HHpred interactive server for protein
857 homology detection and structure prediction. *Nucleic Acids Res* **33**.
858 doi:10.1093/nar/gki408
859 Soldati D, Dubremetz JF, Lebrun M. 2001. Microneme proteins: structural and functional
860 requirements to promote adhesion and invasion by the apicomplexan parasite
861 Toxoplasma gondii. *Int J Parasitol* **31**:1293–1302. doi:10.1016/S0020-
862 7519(01)00257-0

863 Stat M, Carter D, Hoegh-Guldberg O. 2006. The evolutionary history of *Symbiodinium*
864 and scleractinian hosts—Symbiosis, diversity, and the effect of climate change.
865 *Perspect Plant Ecol Evol Syst* **8**:23–43. doi:10.1016/J.PPEES.2006.04.001
866 Supek F, Bošnjak M, Škunca N, Šmuc T. 2011. REVIGO Summarizes and Visualizes
867 Long Lists of Gene Ontology Terms. *PLoS One* **6**:e21800.
868 doi:10.1371/journal.pone.0021800
869 Takabayashi M, Adams LM, Pochon X, Gates RD. 2012. Genetic diversity of free-living
870 Symbiodinium in surface water and sediment of Hawai‘i and Florida. *Coral Reefs*
871 **31**:157–167. doi:10.1007/s00338-011-0832-5
872 Talman AM, Domarle O, McKenzie FE, Ariey F, Robert V. 2004. Gametocytogenesis:
873 The puberty of Plasmodium falciparum. *Malar J*. doi:10.1186/1475-2875-3-24
874 Tchernov D, Gorbunov MY, de Vargas C, Narayan Yadav S, Milligan AJ, Häggblom M,
875 Falkowski PG. 2004. Membrane lipids of symbiotic algae are diagnostic of
876 sensitivity to thermal bleaching in corals. *Proc Natl Acad Sci U S A* **101**:13531–5.
877 doi:10.1073/pnas.0402907101
878 Tchernov D, Kvitt H, Haramaty L, Bibby TS, Gorbunov MY, Rosenfeld H, Falkowski PG.
879 2011. Apoptosis and the selective survival of host animals following thermal
880 bleaching in zooxanthellate corals. *Proc Natl Acad Sci* **108**:9905–9909.
881 doi:10.1073/pnas.1106924108
882 ten Lohuis MR, Miller DJ. 1998. Hypermethylation At Cpg-Motifs in the Dinoflagellates
883 Amphidinium Carterae (Dinophyceae) and Symbiodinium Microadriaticum
884 (Dinophyceae): Evidence From Restriction Analyses, 5-Azacytidine and Ethionine
885 Treatment. *J Phycol* **34**:152–159. doi:10.1046/j.1529-8817.1998.340152.x

886 Valmsen K, Järving I, Boeglin WE, Varvas K, Koljak R, Pehk T, Brash AR, Samel N.
887 2001. The origin of 15R-prostaglandins in the Caribbean coral Plexaura
888 homomalla: molecular cloning and expression of a novel cyclooxygenase. *Proc Natl*
889 *Acad Sci U S A* **98**:7700–7705. doi:10.1073/pnas.131022398
890 Wangpraseurt D, Larkum AWD, Ralph PJ, Kühl M. 2012. Light gradients and optical
891 microniches in coral tissues. *Front Microbiol* **3**:316. doi:10.3389/fmicb.2012.00316
892 Weinheimer AJ, Spraggins RL. 1969. The occurrence of two new prostaglandin
893 derivatives (15-epi-PGA2 and its acetate, methyl ester) in the Gorgonian
894 PlexauraHomomalla Chemistry of Coelenterates. XV. *Tetrahedron Lett* **10**:5185–
895 5188. doi:10.1016/S0040-4039(01)88918-8
896 Weis V. 2008. Cellular mechanisms of Cnidarian bleaching: stress causes the collapse
897 of symbiosis. *J Exp Biol*.
898 Wilkens S. 2015. Structure and mechanism of ABC transporters. *F1000Prime Rep* **7**:14.
899 doi:10.12703/P7-14
900 Wood DE, Salzberg SL. 2014. Kraken: ultrafast metagenomic sequence classification
901 using exact alignments. *Genome Biol* **15**:R46. doi:10.1186/gb-2014-15-3-r46
902 Xiang T, Nelson W, Rodriguez J, Tolleter D, Grossman AR. 2015. *Symbiodinium*
903 transcriptome and global responses of cells to immediate changes in light intensity
904 when grown under autotrophic or mixotrophic conditions. *Plant J* **82**:67–80.
905 doi:10.1111/tpj.12789
906 Zhang H, Hou Y, Miranda L, Campbell DA, Sturm NR, Gaasterland T, Lin S. 2007.
907 Spliced leader RNA trans-splicing in dinoflagellates. *Proc Natl Acad Sci* **104**:4618–
908 4623. doi:10.1073/pnas.0700258104

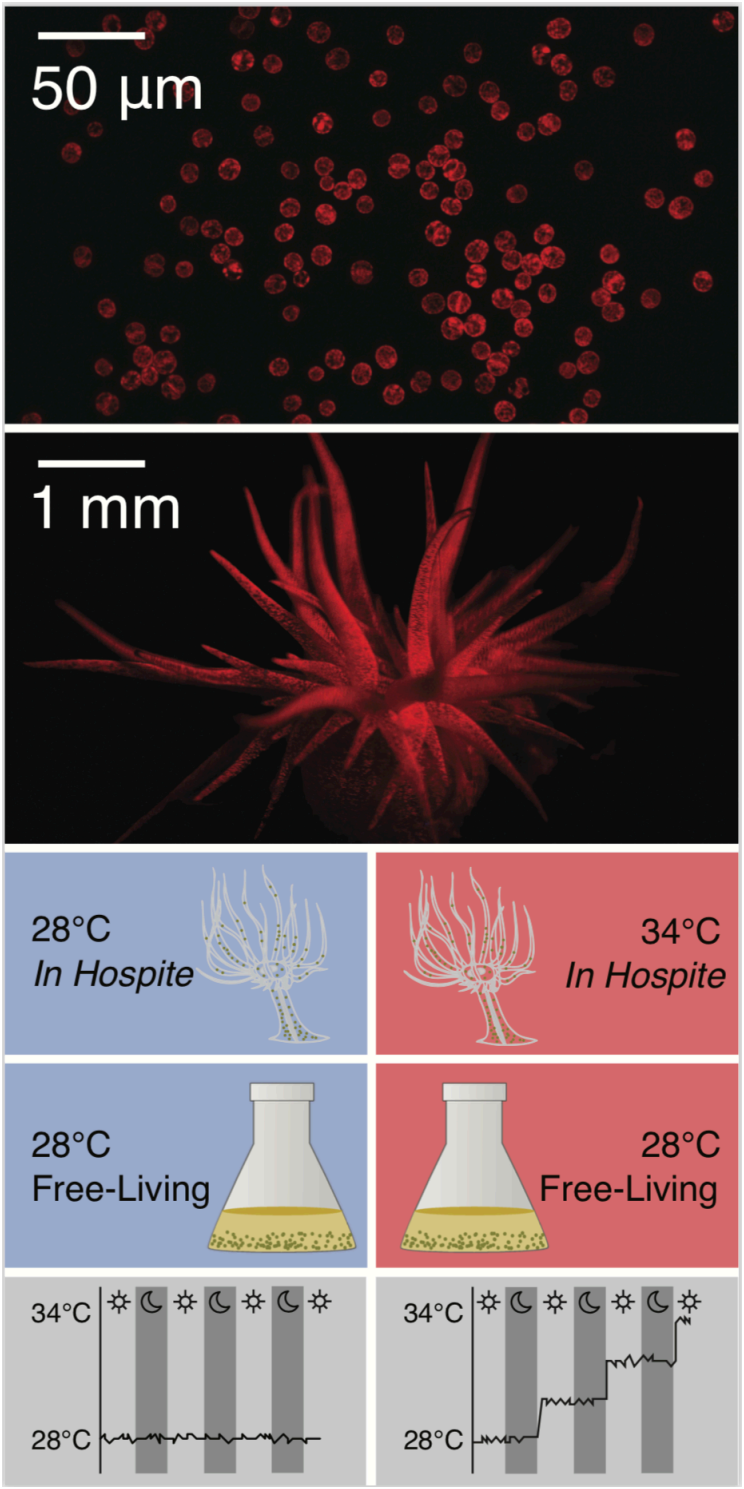

Figure 1: *Durusdinium trenchii* in free-living culture state (top) and *in hospite* in *E. pallida* (second panel). Schematic of experimental treatments (lower panels) comparing symbiotic state and thermal stress, with temperature and light profiles.

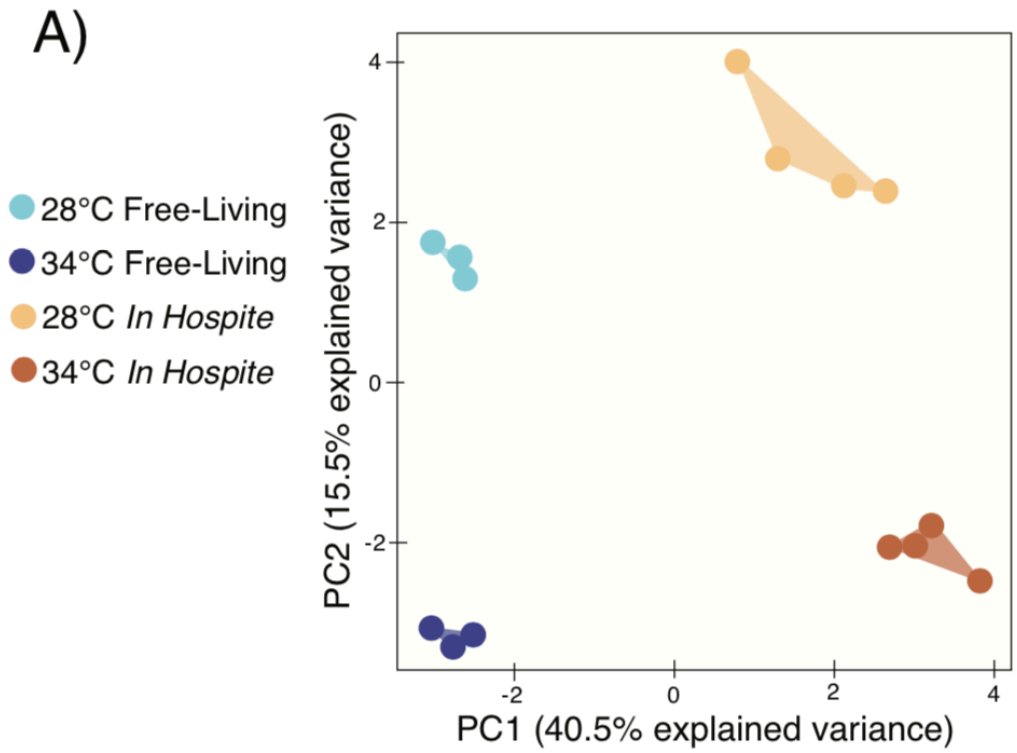

B)

		#Transcripts driving PC (jackstraw)	#Transcripts DE (edgeR)	#Transcripts DE & driving PC
PC1 (*In Hospite* vs. Free-Living)	@ 28°C	11,933	1,993	104
	@ 34°C		3,592	525
PC2 (34°C vs. 28°C)	Symbiotic	11,904	709	39
	Free-living		353	28

Figure 2. A) Principal component analysis depicting the ordination of biological replicates by all analyzed transcripts. (B) Summary of the number of transcripts driving PC1 and PC2, the number of transcripts DE according to edgeR, and the number of transcripts that were both DE and significant drivers of PC1 and PC2.

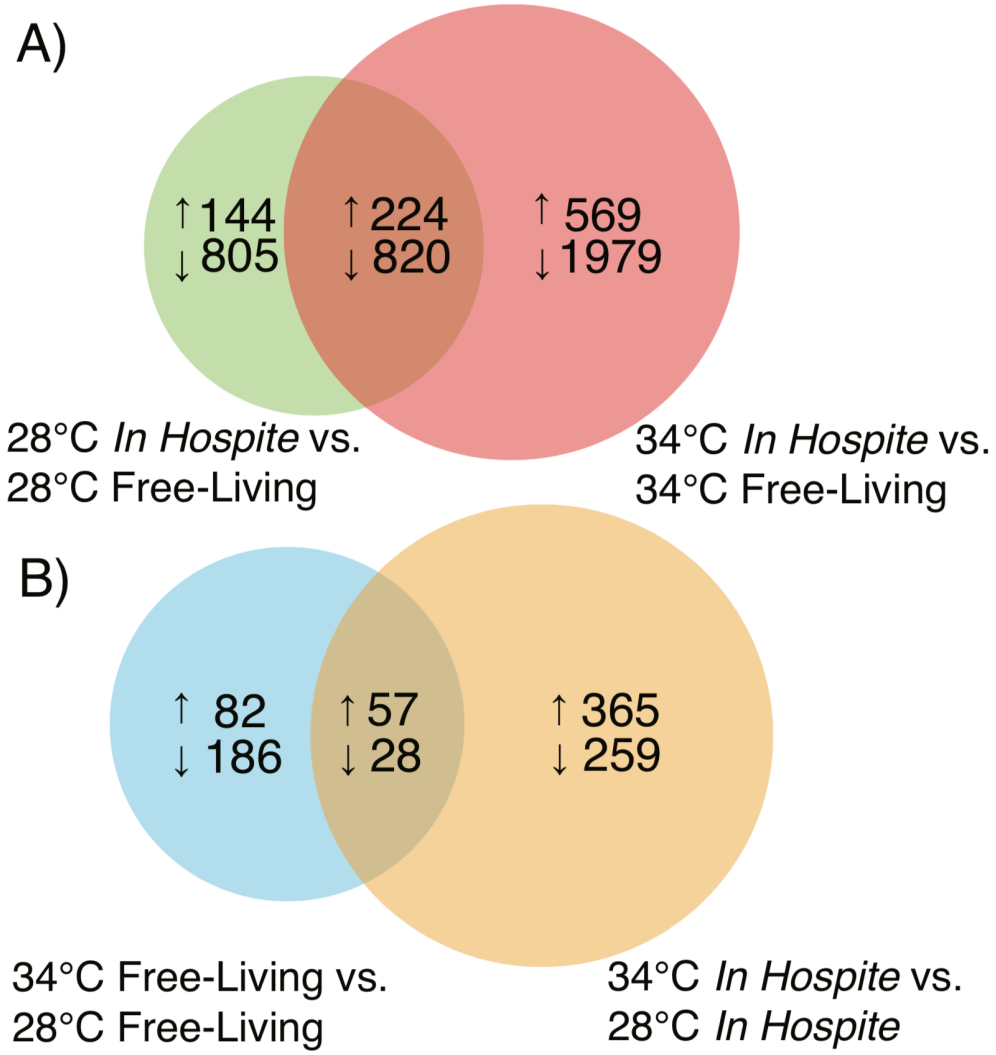

Figure 3. Venn diagrams of the number of differentially expressed transcripts by pairwise comparison (FDR-corrected $p < 0.01$, greater than 2-fold difference). A) Contrasts transcriptional changes between *in hospite* and free-living transcripts at 28°C and 34°C. B) Comparison of transcripts differentially expressed in the free-living and *in hospite* condition, with the core heat stress response represented by the overlapping region.

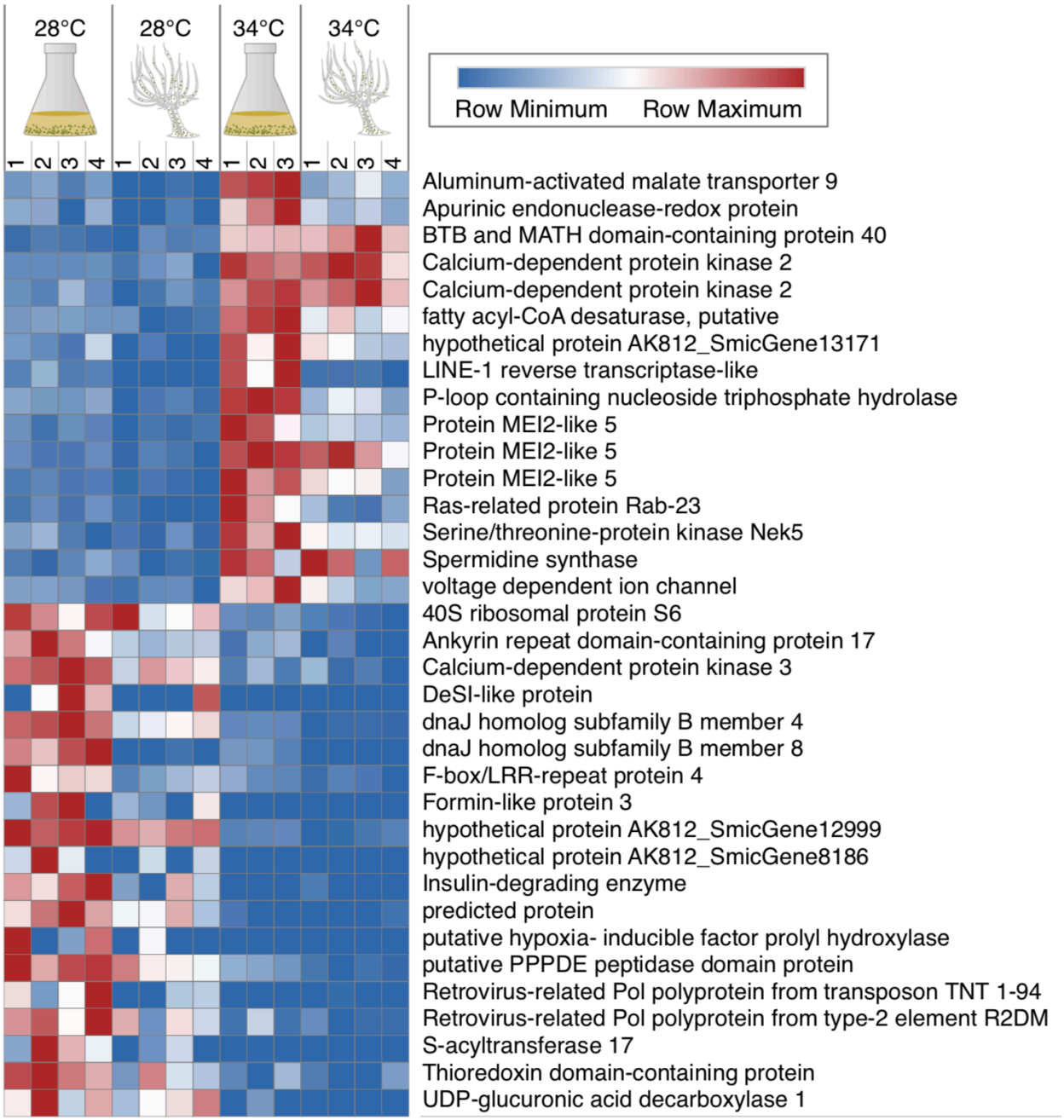

Figure 4. Core heat stress response transcripts. The heatmap reflects annotated transcripts differentially expressed in both *in hospite* and free-living thermal stress conditions. (Unannotated transcripts omitted.)

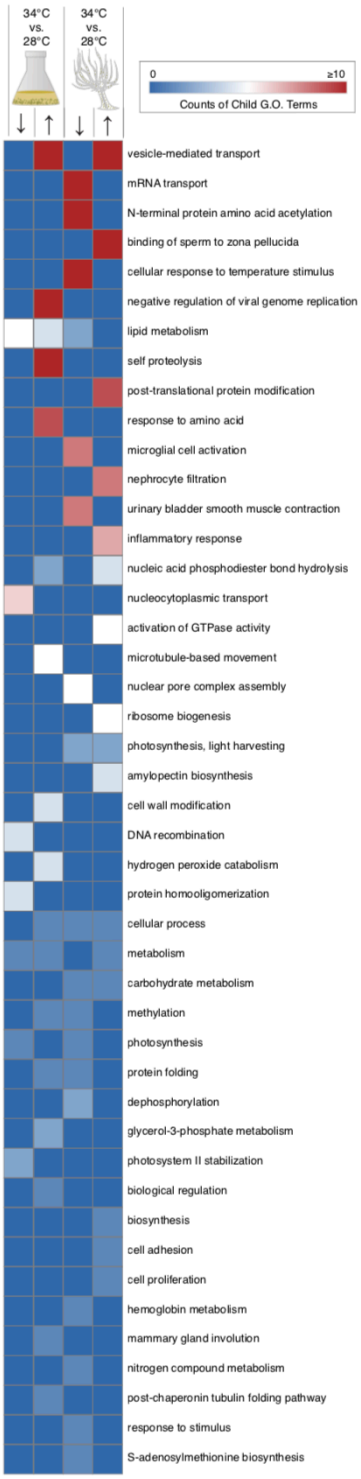

Figure 5. Counts of GO terms enriched exclusively in the free-living and *in hospite* heat stress response. (Terms associated with transcripts differentially expressed in both *in hospite* and free-living conditions were excluded from this enrichment analysis).

Figure 6. Counts of GO terms associated with up- and downregulated transcripts across all comparisons. Parent GO terms are listed for all categories with a minimum sum of two daughter terms across all comparisons.

Supplement 1

Supplemental Materials and Methods

Experimental Overview

Briefly, the experimental design compares *D. trenchii* in the free-living state (culture) and *in hospite* in an *Exaiptasia* host under two different temperature regimens, a steady-state culture temperature of 28°C and a thermal stress of 34°C, both under light intensity levels of 80 µE. Four biological replicates of each condition were implemented, with replication performed in time.

Exaiptasia symbiont manipulation and *Symbiodinacaea* culture

Aposymbiotic *Exaiptasia* were produced through repeated cold treatment (8 hours at 4°C, repeated three times over the course of one week) followed by DCMU treatment (50 uM) performed for 6 hours with 1000 µmol m−2 s−1 light intensity, repeated twice weekly for 3 weeks. Absence of dinoflagellates was confirmed with fluorescent microscopy. *D. trenchii* strain CCMP2556 was obtained from the National Center for Marine Algae and Microbiota (East Boothbay, Maine) and cultured in Prov50 media under a 12:12 light cycle. Log phase cultures were used for all experiments. Aposymbiotic anemones were challenged with 100,000 log phase *Durusdinium trenchii* cells combined with freshly hatched *Artemia franciscana* in a total volume of 10 ml of sterile seawater, with water replaced after 12 hours . Infection was confirmed by fluorescent microscopy, followed by PCR and sequencing of 23S. Anemones hosting *D. trenchii* were grown for one year prior to experimental manipulation with light levels at

964 approximately 80 μmol m−2 s−1. Anemones were fed freshly hatched *Artemia* twice
965 weekly.

966 **Symbiosis state comparison and thermal challenge**

967 To inform the design of this experiment, maximum quantum yield in cultured *D.*
968 *trenchii* was assessed through time, at temperatures from 28 to 36° C (n=3) using a
969 PAM fluorometer (Walz, Germany). We found that the rapid decline in maximum
970 quantum yield began at 34°C at 2 hours of thermal stress. In an 8 hour timespan, we did
971 not find significant decline at the lower thermal treatments.

972 Anemones and cultures were maintained at 28°C with 80 μmol m−2 s−1
973 irradiance and ramped up to the 34° C challenge at a rate of 2°C per day for thermal
974 stress treatments. Mid-photoperiod (6 hours into light phase of the diel cycle), samples
975 were frozen for subsequent RNA extraction. Log phase *D. trenchii* cultures were used
976 for all experiments. Replicates were performed in time, with one replicate of each
977 treatment included in each trial. A total of four biological replicates were collected for
978 each treatment.

979 **Symbiodinacaea RNA Extraction Enrichment Protocol**

980 Anemones were frozen in minimal seawater in 2 ml cryotubes in liquid nitrogen
981 and stored at -80°C till extraction. For enrichment of Symbiodiniaceae from anemone
982 extractions, 500 ul of Buffer RLT with 0.1% 2-mercaptoethanol (Qiagen) was added to
983 each tube and manually flicked till frozen tissue was dislodged and decanted into 1.5 ml
984 centrifuge tube. Tissue was gently homogenized with a plastic pestle and vortexed at
985 maximum speed for 1 minute. Homogenate was centrifuged at 10,000 g for 3 min. Clear
986 supernatant was carefully removed and discarded, leaving the symbiont pellet intact.

987 This pellet was resuspended in 1.4 ml of Buffer RLT and vortexed till the mixture was
988 homogenous. This suspension was centrifuged at 3,000 g for 3 min. Clear supernatant
989 was discarded, and an additional 1.4 ml of Buffer RLT was added vortexed till
990 homogenous. This was centrifuged at 3,000 g for 3 minutes and clear supernatant was
991 discarded prior to resuspension in 600 ul Buffer RLT. Contents were transferred to a
992 screw top 2.0 ml tube and bead beat for 1 min at 6 m/s with glass beads. Homogenate
993 was processed with the Qiagen RNeasy Kit as per manufacturer instructions, with an
994 additional RPE Buffer wash prior to elution of total RNA. Symbiodiniaceae were snap
995 frozen in liquid nitrogen and extracted alongside anemone tissue, implementing an
996 identical washing scheme to eliminate any extraction-based bias.

997 **Library Construction and Sequencing**

998 Following poly(A) selection from total RNA, RNAseq libraries were constructed
999 from mRNA using the NEBNext Ultra Directional RNA Library Prep Kit (NEB). A total of
1000 16 libraries were sequenced on two Illumina HiSeq lanes, using v4 150 base pair
1001 paired-end chemistry (Illumina). The indexed samples were pooled across both lanes to
1002 eliminate lane effects. Raw data have been archived on the SRA and is available under
1003 NCBI TSA BioProject PRJNA508937.

1004 ***De novo* transcriptome assembly**

1005 Quality of the resulting raw reads were assessed via FastQC and low-quality
1006 reads were removed and/or trimmed with Trimmomatic (Bolger et al., 2014) with a
1007 minimum read length threshold of 50 bp. Trimmed reads that aligned concordantly
1008 against the human and *Exaiptasia pallida* genomes using the HISAT2 (Kim et al., 2015)
1009 program to remove any contaminating eukaryotic reads. Remaining reads were then

1010 filtered using all bacterial, archaeal, and viral genomes present in RefSeq (as of Sep. 8,
1011 2017) using Kraken, an ultra-fast taxonomic sequence classification program (Wood
1012 and Salzberg, 2014). The 526,545,945 remaining PE reads were then assembled with
1013 Trinity v2.4.2 (Grabherr et al., 2011) with a minimum contig length of 200 bp.
1014 Redundant contigs were removed using uCLUST (Edgar, 2010) at an identity
1015 threshold of 100%. Removal of eukaryotic contaminants via Hisat2 and prokaryotic
1016 contigs via Kraken (Wood and Salzberg, 2014) was repeated once more on the
1017 transcriptome assembly to remove any lingering contamination that could not be
1018 identified from the raw reads. Ribosomal RNA contamination was identified and
1019 removed by aligning transcriptome contigs against all of the SILVA rRNA databases
1020 (Quast et al., 2012) with Bowtie2 (Langmead and Salzberg, 2012) resulting in a final
1021 assembly of 85,130 contigs. Assembly statistics were calculated using Transrate
1022 (Smith-Unna et al., 2016) (Supplementary Table 1).
1023 For annotation, the assembly was searched against the NR protein database
1024 using DIAMOND, a fast search algorithm that employs double-indexing and spaced
1025 seeds of various weights and shape to make it ~20,000x faster than BLASTX with
1026 comparable level of sensitivity and accuracy (Buchfink et al., 2015). These results were
1027 input into with Trinotate using BLASTP and BLASTX searches against the SwissProt
1028 and Uniref90 databases with an e-value cutoff of $< 1 \times 10^{-5}$. Open reading frames
1029 (ORFs) were predicted using Transdecoder under the default settings. Gene ontology
1030 classifications were extracted from search results against the SwissProt database. The
1031 searches were conducted using DIAMOND, a fast search algorithm that employs
1032 double-indexing and spaced seeds of various weights and shape to make it ~20,000x

1033 faster than BLAST with a similar sensitivity and accuracy (Buchfink et al., 2015).
1034 Additional annotation was performed using Blast2GO (Conesa et al., 2005), with
1035 redundant GO terms removed with a custom script.
1036 Quality-controlled reads were mapped back to the final assembly using Salmon
1037 at an average mapping rate of 88% and 30.1 million reads per sample. Mapping results
1038 were imported into R for differential gene expression analysis with the edgeR package
1039 (Robinson et al., 2010). Low-count transcripts that across all samples with a mapping
1040 rate of < 10 reads were removed prior to count normalization within R. Differential gene
1041 expression anlysis was then performed in edgeR using a generalized linear model to
1042 determine the effects of temperature and symbiotic state as well as the interaction
1043 between the two on changes in gene expression. Four pairwise comparisons were then
1044 conducted using the GLM: (1) free-living at 28 °C vs. free-living at 34 °C (2) symbiotic at
1045 28°C vs. symbiotic at 34 °C (3) free-living at 28 °C vs. symbiotic at 28 °C and (4) free-
1046 living at 34 °C and symbiotic at 34 °C. An additional comparison with the GLM was done
1047 using the formula ((symbiotic at 34 °C vs. free-living at 34 °C) - (free-living at 28 °C vs.
1048 symbiotic at 28 °C)) to determine genes that were differentially expressed in response
1049 to symbiosis but responded differently to temperature. Results from each of the five
1050 comparisons in edgeR were then used for gene ontology (GO) enrichment analyses
1051 within the R package topGO. GO results for the different comparisons were summarized
1052 and viewed using the web-based REVIGO program (Supek et al., 2011).
1053

1054 # Supplement 1 (Supporting Figures and Tables)

1055

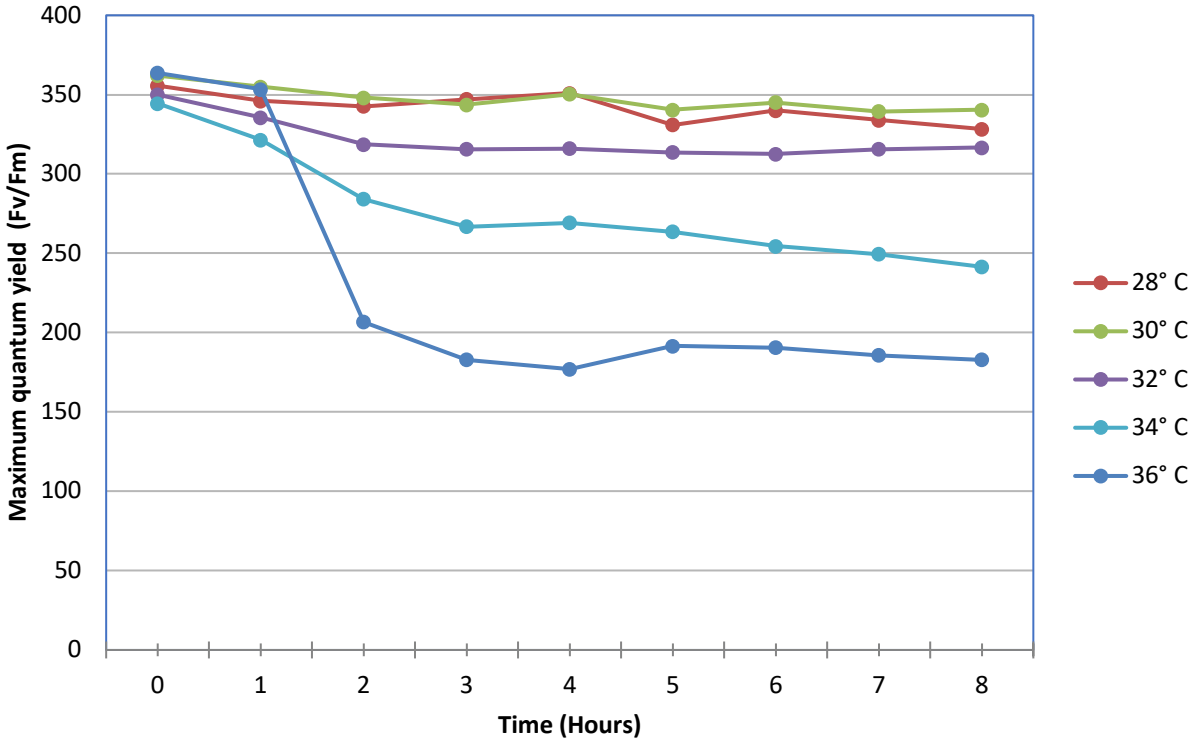

1056

1057 **Supplementary Figure 1.** Maximum quantum yield of *D. trenchii* cultures assessed via

1058 PAM fluorometry throughout a thermal stress timecourse.

1059

1060

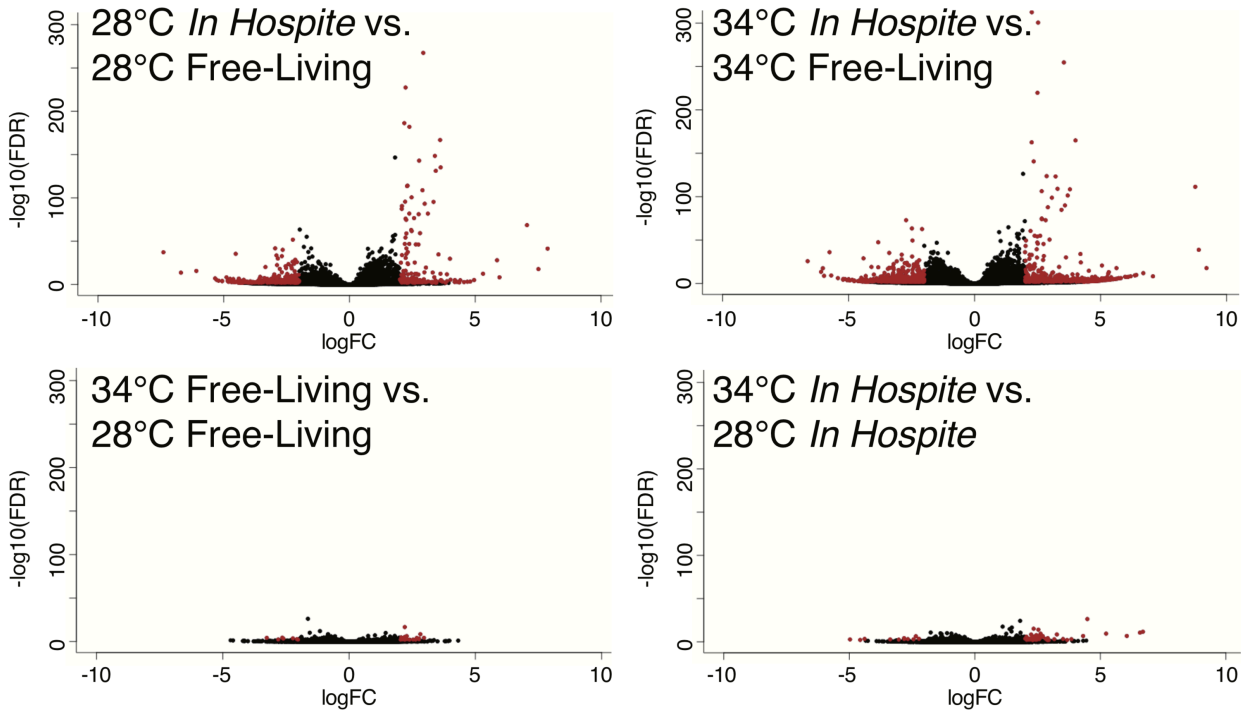

Supplementary Figure 2. Volcano plots of all transcripts; transcripts with FDR corrected p-value < 0.01 and greater than $\log_2$ 2-fold difference are indicated in red.

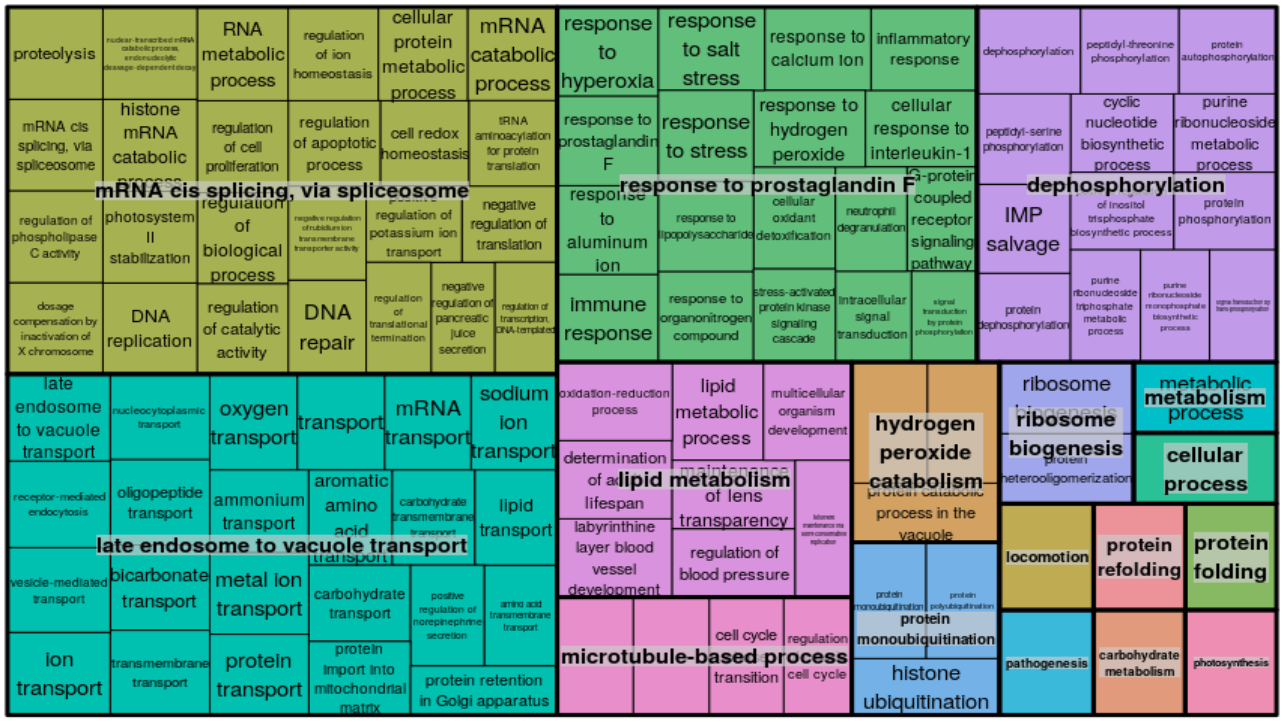

Supplementary Figure 3. REVIGO tree diagram summary of the GO terms associated with transcripts up-regulated in response to symbiosis compared to free-living *D. trenchii* at 28 °C.

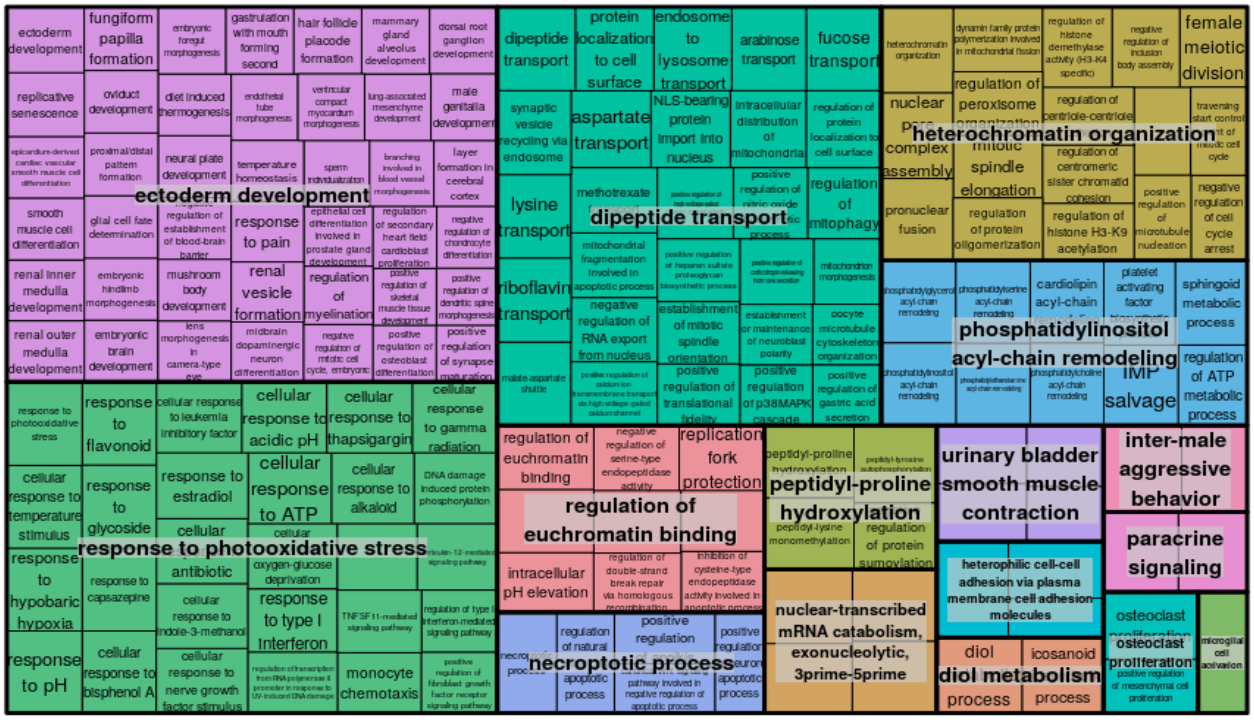

Supplementary Figure 4. REVIGO tree diagram summary of the GO terms associated with transcripts down-regulated in response to symbiosis compared to free-living *D. trenchii* at 28 °C.

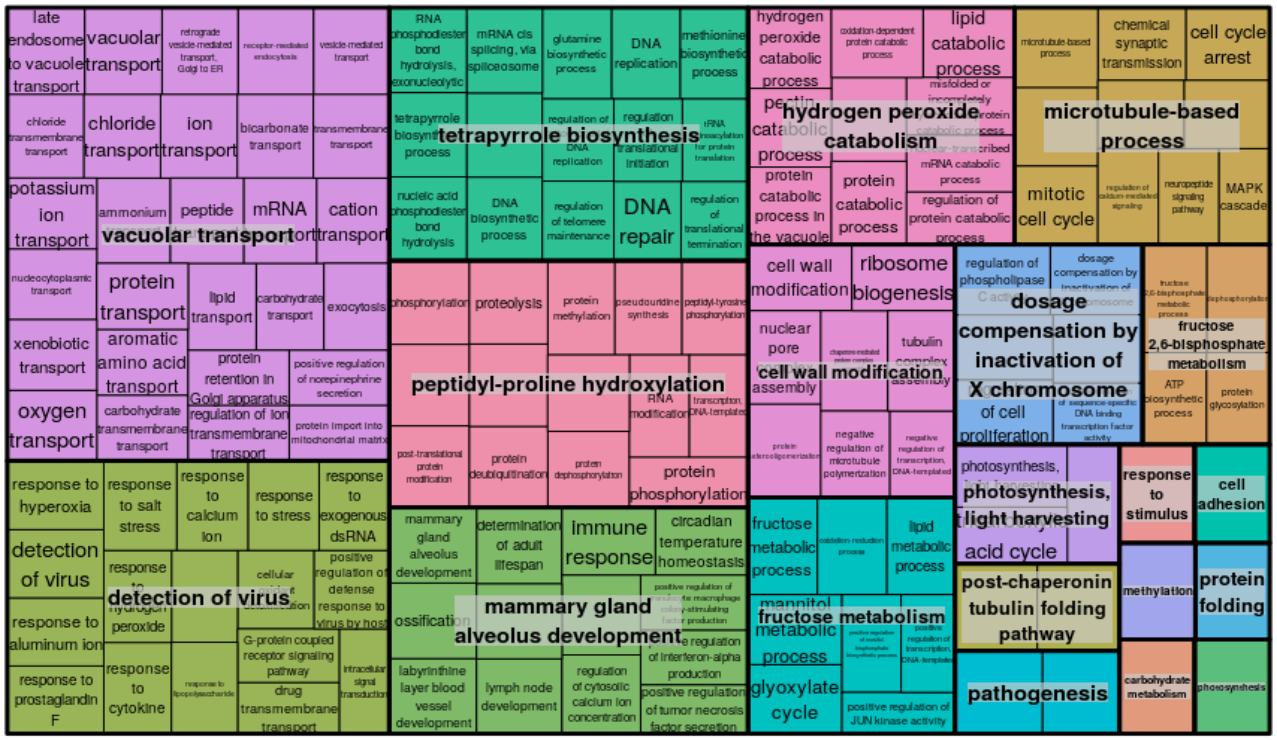

Supplementary Figure 5. REVIGO tree diagram summary of the GO terms associated with transcripts up-regulated in response to symbiosis compared to free-living *D. trenchii* at 34 °C.

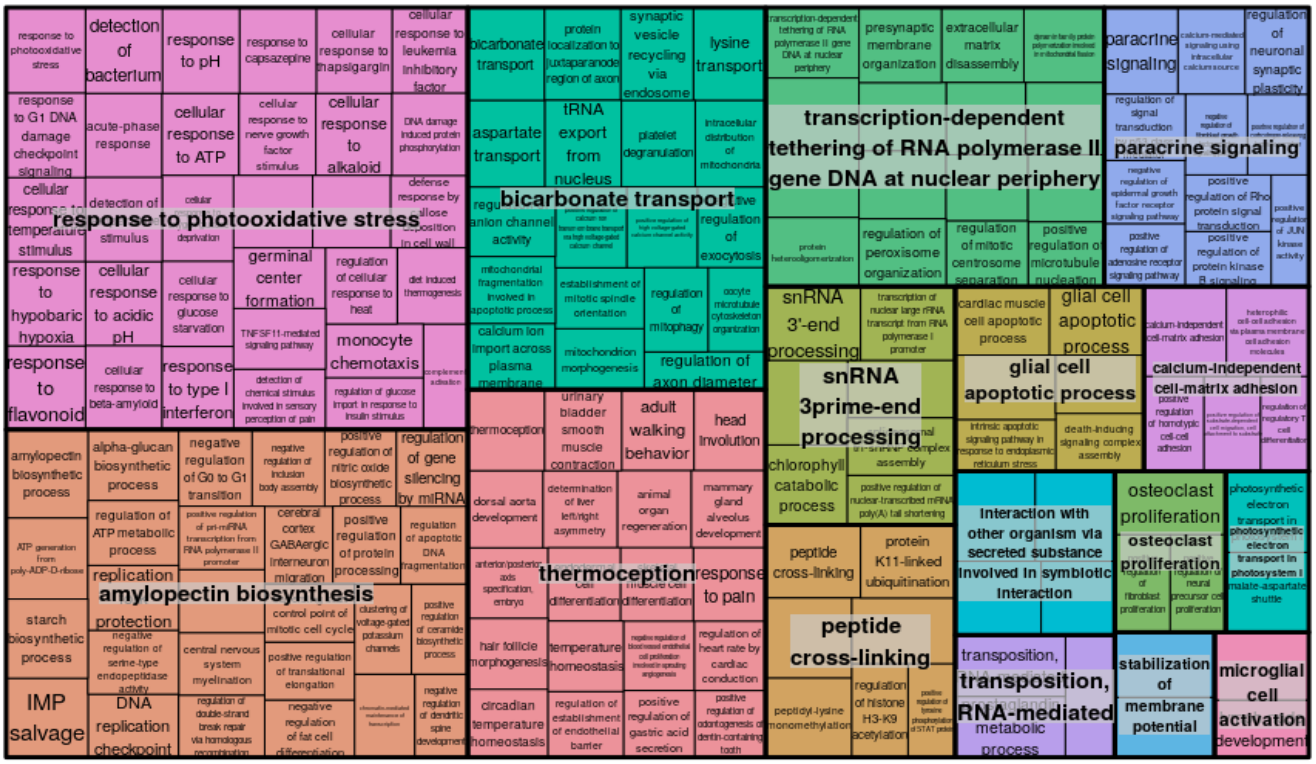

Supplementary Figure 6. REVIGO tree diagram summary of the GO terms associated with transcripts down-regulated in response to symbiosis compared to free-living *D. trenchii* at 34 °C.

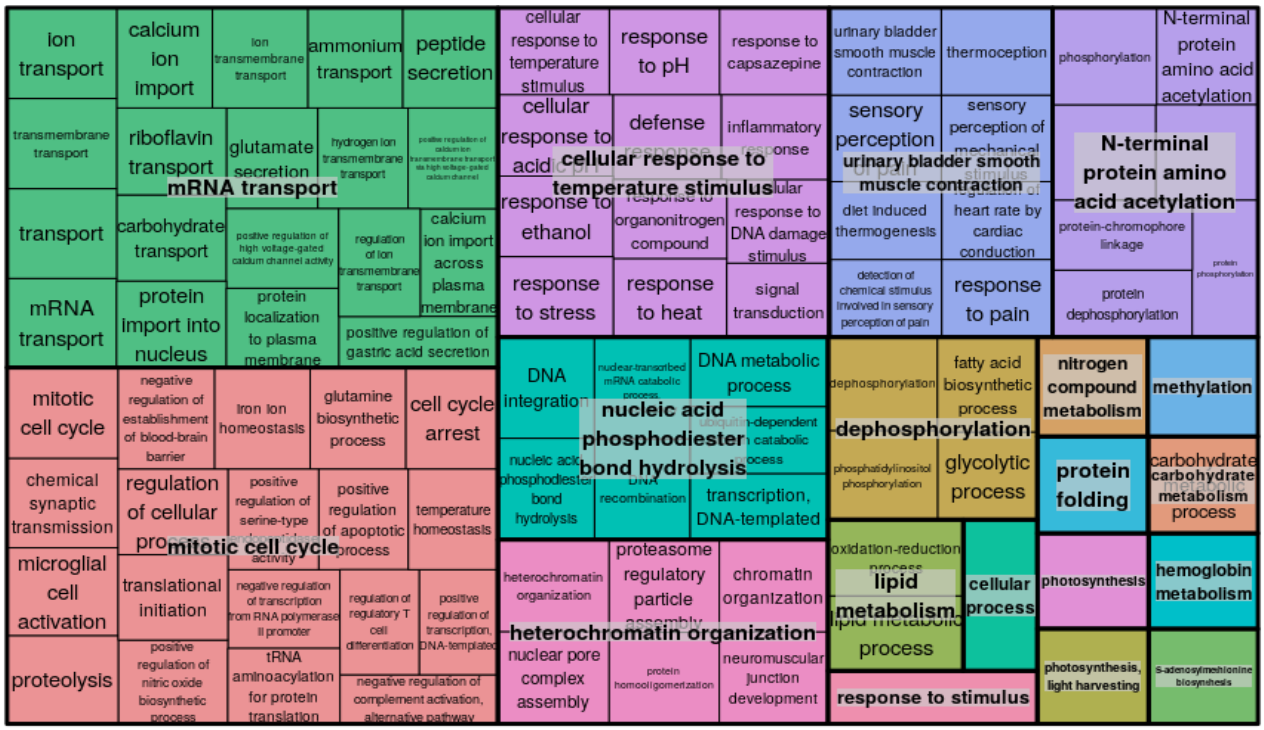

Supplementary Figure 7. REVIGO tree diagram summary of the GO terms associated with transcripts up-regulated in response to temperature stress in *in hospite D. trenchii* at 34 °C.

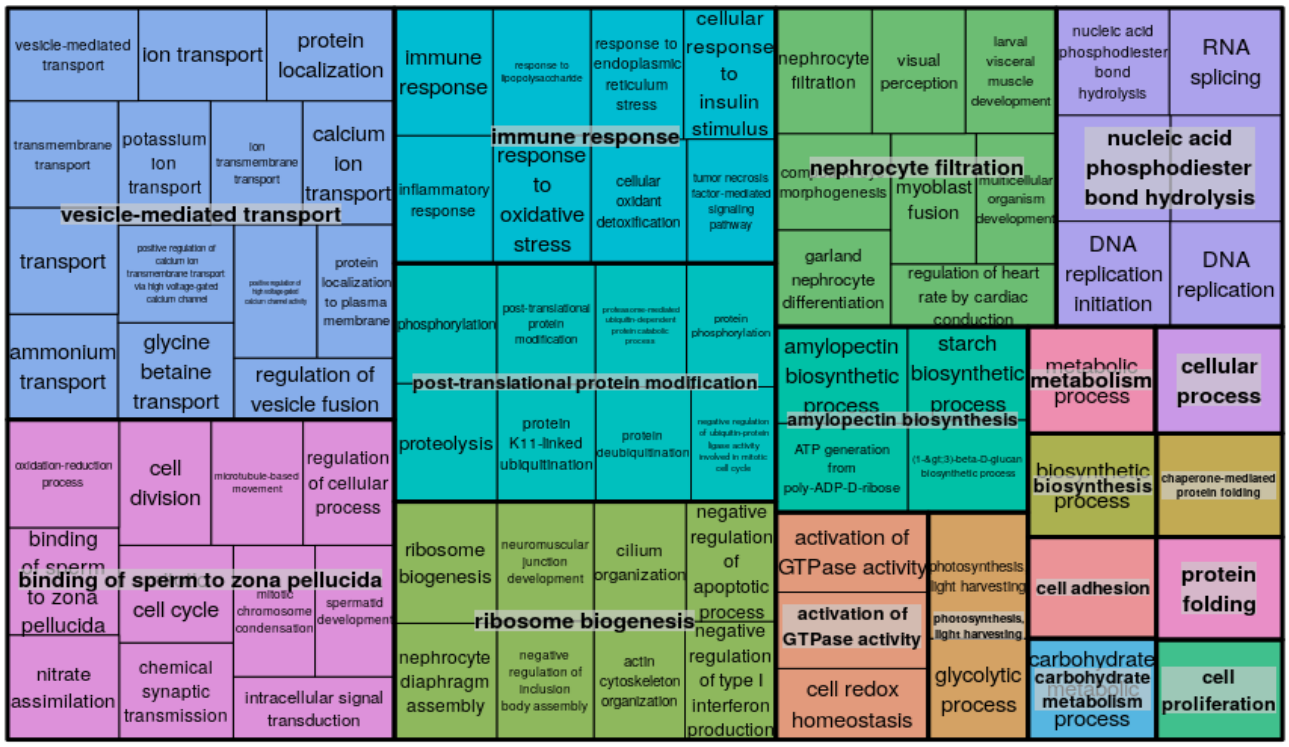

Supplementary Figure 8. REVIGO tree diagram summary of the GO terms associated with transcripts down-regulated in response to temperature stress in *in hospite D. trenchii* at 34 °C.

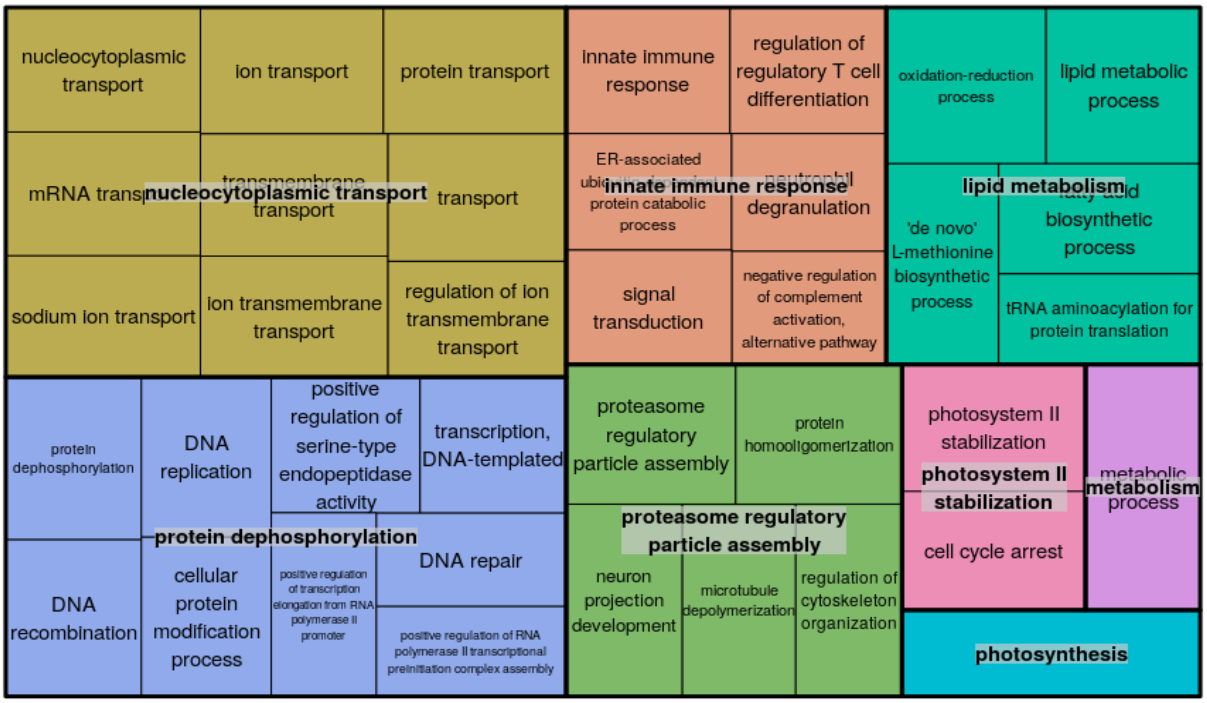

Supplementary Figure 9. REVIGO tree diagram summary of the GO terms associated with transcripts up-regulated in response to temperature stress in free-living *D. trenchii* at 34 °C.

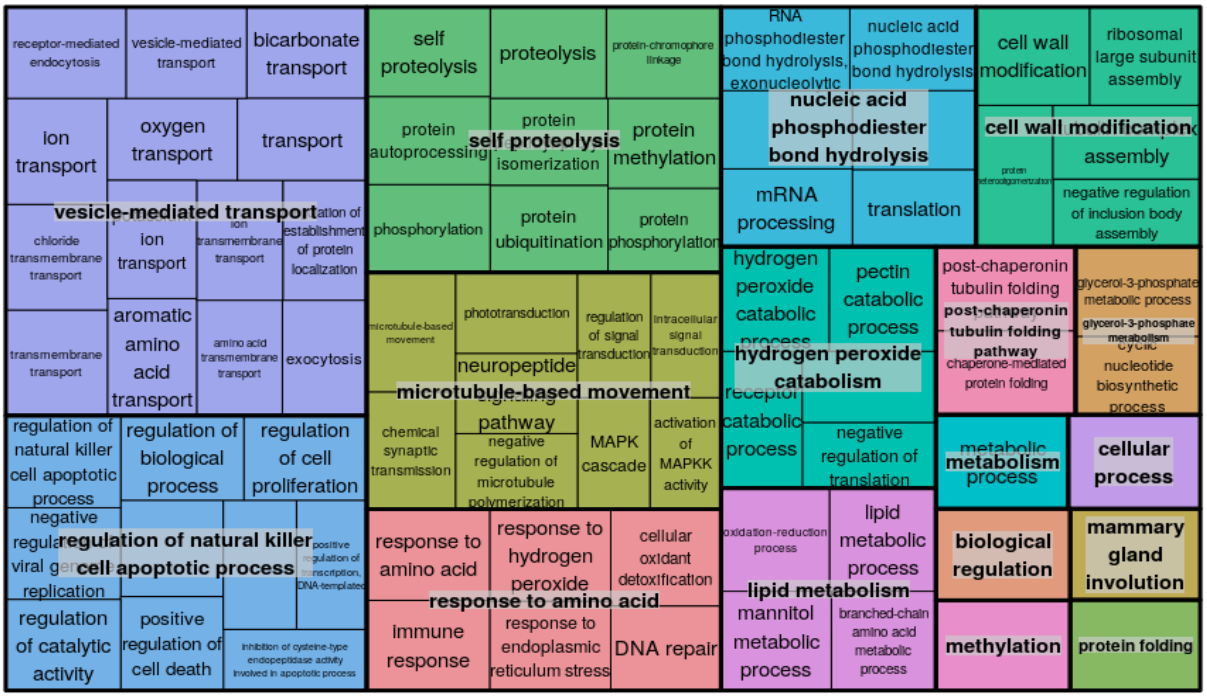

Supplementary Figure 10. REVIGO tree diagram summary of the GO terms associated with transcripts down-regulated in response to temperature stress in free-living *D. trenchii* at 34 °C.

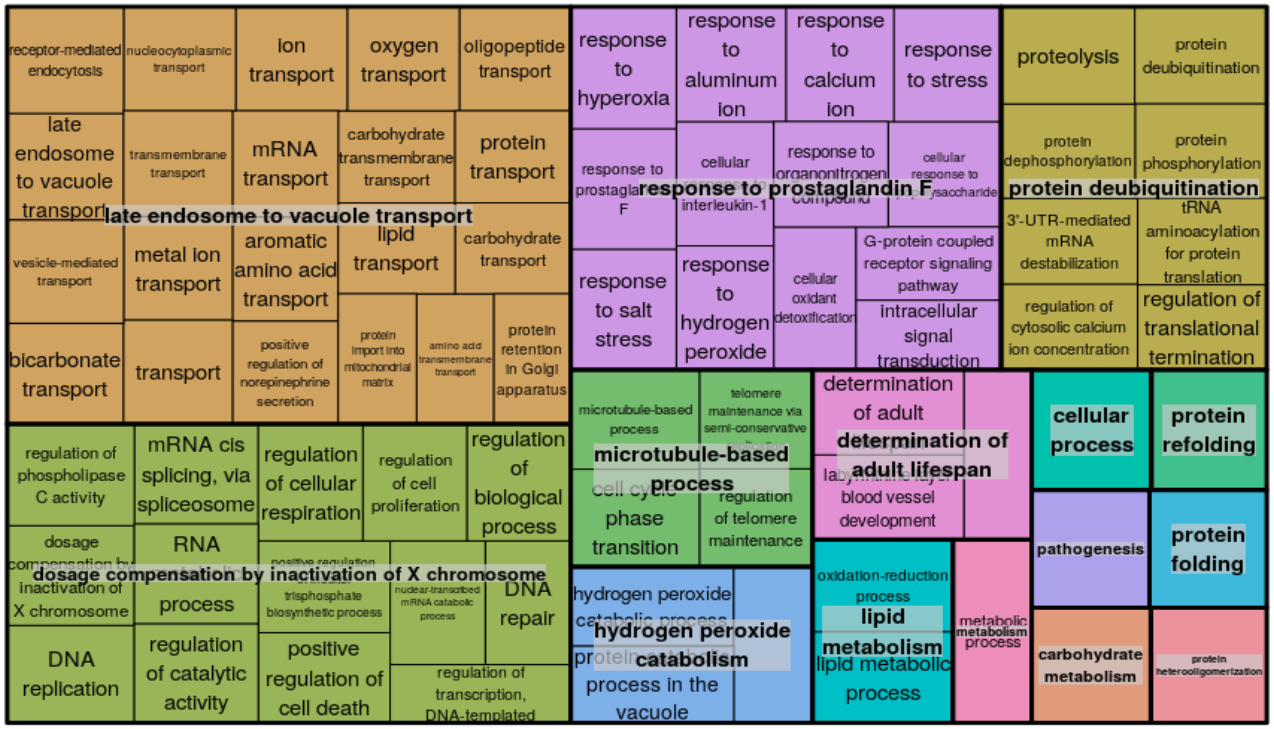

Supplementary Figure 11. REVIGO tree diagram summary of the GO terms associated with transcripts that were up-regulated in response to symbiosis in *D. trenchii* at both 28 °C and 34 °C.

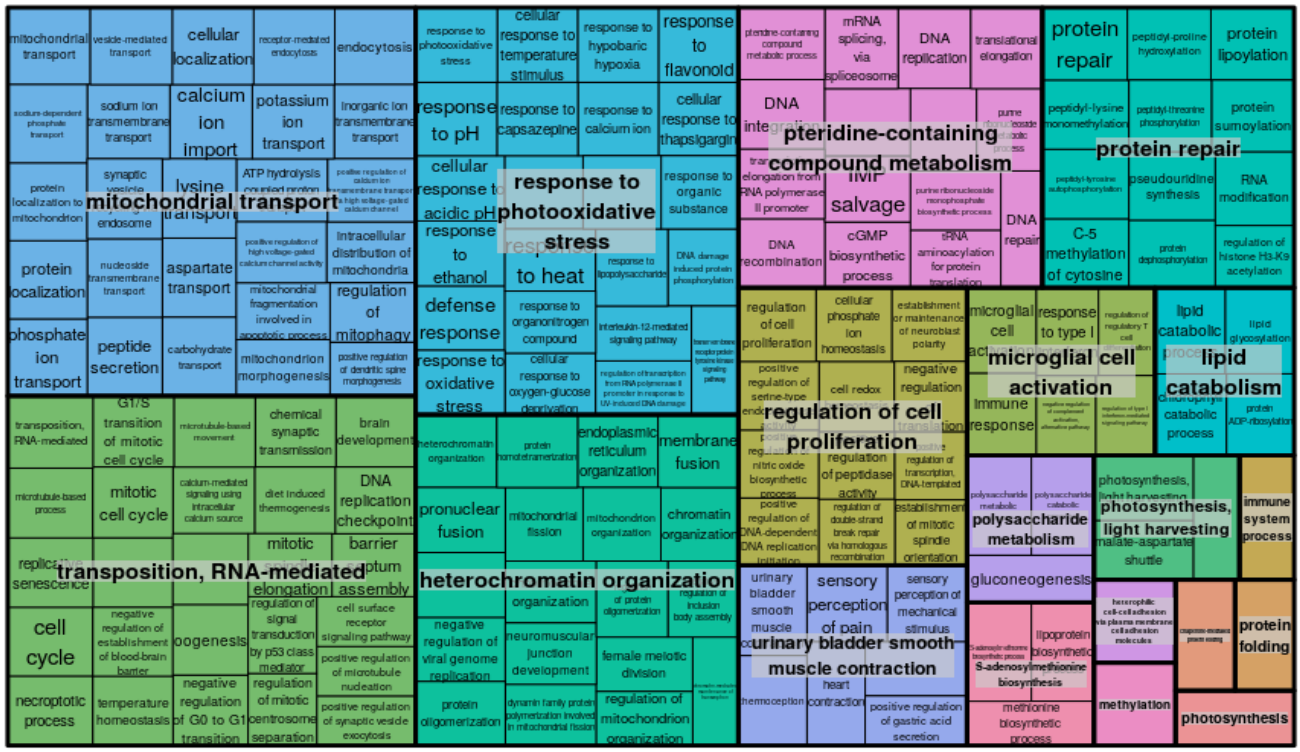

1115

1116 **Supplementary Figure 12.** REVIGO tree diagram summary of the GO terms

1117 associated with transcripts that were down-regulated in response to symbiosis in *D.*

1118 *trenchii* at both 28 °C and 34 °C.

1119

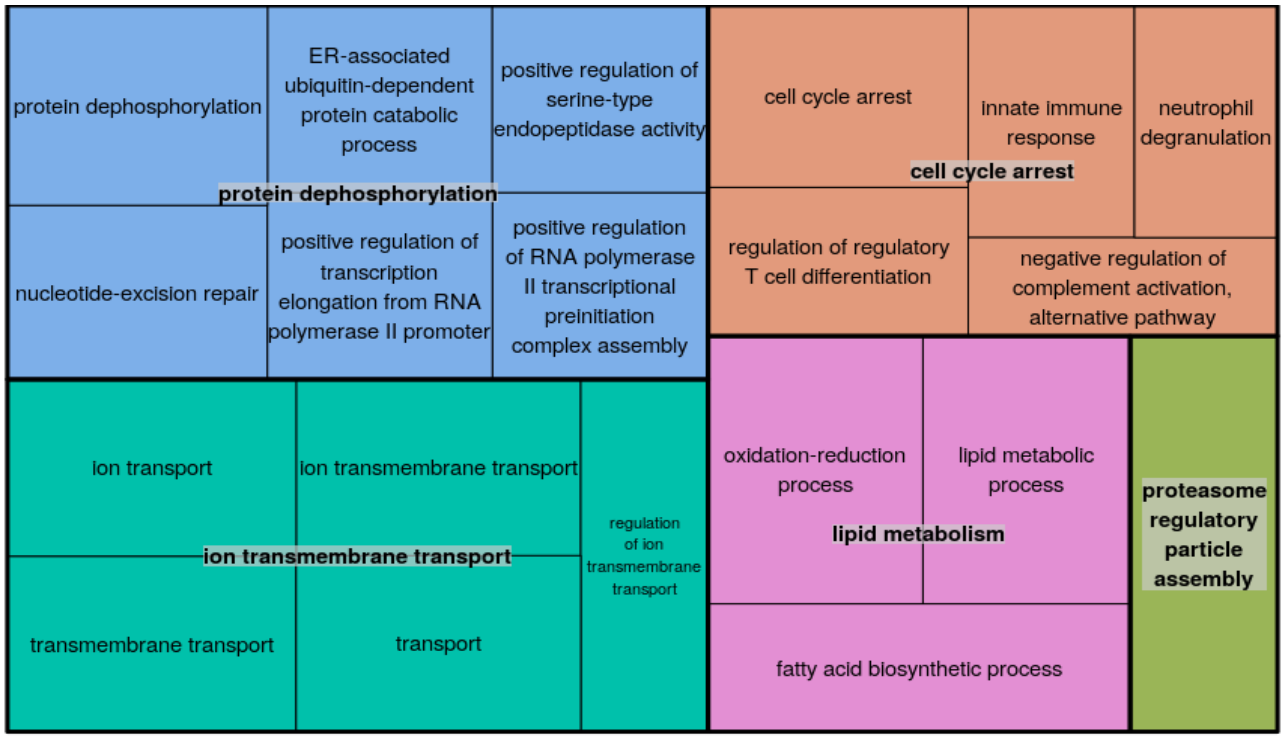

Supplementary Figure 13. REVIGO tree diagram summary of the GO terms associated with transcripts that were up-regulated in response to temperature stress in both free-living and symbiotic *D. trenchii*.

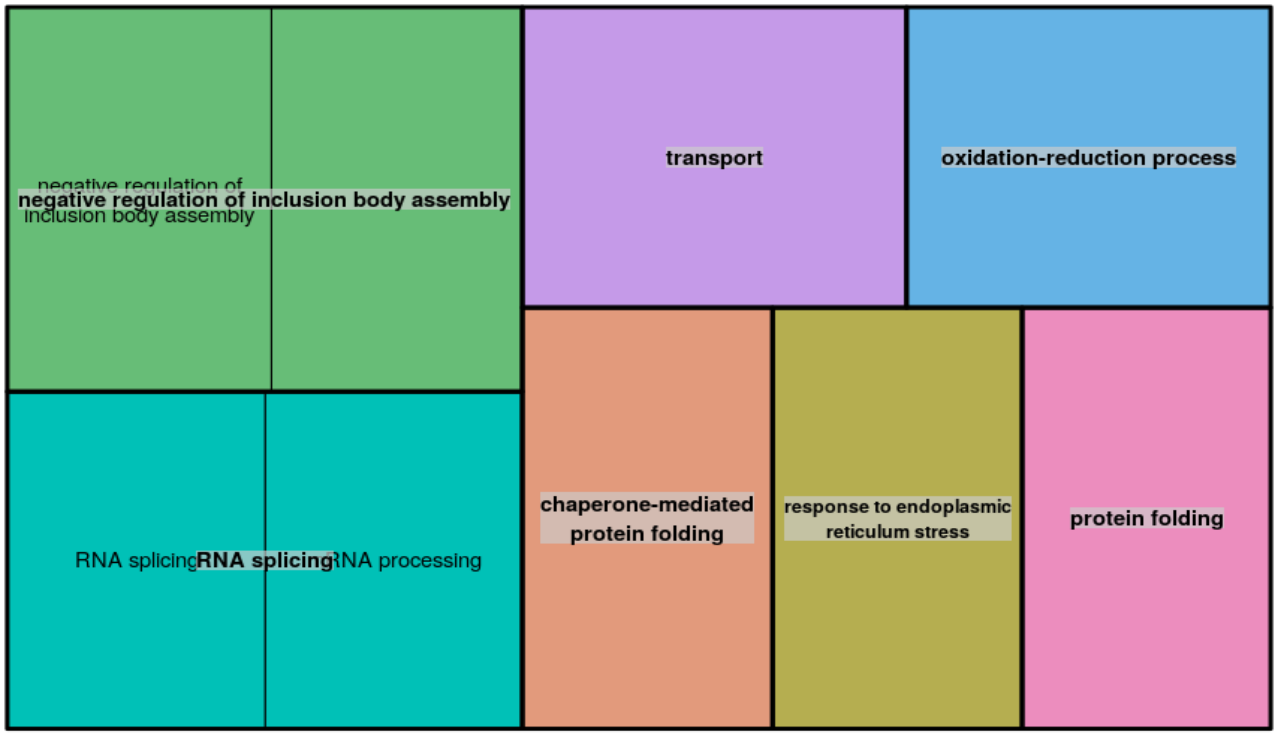

Supplementary Figure 14. REVIGO tree diagram summary of the GO terms associated with transcripts that were down-regulated in response to temperature stress in both free-living and symbiotic *D. trenchii*.

1128

Assembly metrics	
Total PE read sets after QC	526,545,945
Total PE read sets after QC (%)	81.5%
Assembly length (Mbp)	81.7
# Transcripts	85,168
Predicted ORF count	47,335
Genes annotated	28,531
Genes annotated (%)	60.3%
Longest gene length (bp)	8,088
Mean gene length (bp)	960.36
N50 (bp)	1,470
GC content (%)	0.55

1129

1130 **Supplementary Table 1.** Assembly statistics for the *D. trenchii* assembly

1131

1132

GO ID	Term	Annotated	Significant	FDR
GO:0003374	dynamin family protein polymerization involved in mitochondrial fission	6	3	0.0001
GO:0007089	traversing start control point of mitotic cell cycle	2	2	0.0003
GO:0018107	peptidyl-threonine phosphorylation	14	3	0.0017
GO:1904146	positive regulation of meiotic cell cycle process involved in oocyte maturation	4	2	0.0018
GO:0044341	sodium-dependent phosphate transport	5	2	0.0029
GO:0031649	heat generation	60	4	0.003
GO:0002024	diet induced thermogenesis	17	3	0.003
GO:0048266	behavioral response to pain	17	3	0.003
GO:0050960	detection of temperature stimulus involved in thermoreception	17	3	0.003
GO:0050965	detection of temperature stimulus involved in sensory perception	17	3	0.003
GO:0060083	smooth muscle contraction involved in micturition	17	3	0.003

GO:0060454	positive regulation of gastric acid secretion	17	3	0.003
GO:0071318	cellular response to ATP	17	3	0.003
GO:0071502	cellular response to temperature stimulus	17	3	0.003
GO:1901594	response to capsazepine	17	3	0.003
GO:0043154	negative regulation of cysteine-type endopeptidase activity involved in apoptotic process	18	3	0.0035
GO:0071468	cellular response to acidic pH	18	3	0.0035
GO:0090212	negative regulation of establishment of blood-brain barrier	18	3	0.0035
GO:0098703	calcium ion import across plasma membrane	18	3	0.0035
GO:0014047	glutamate secretion	19	3	0.0041
GO:0060337	type I interferon signaling pathway	19	3	0.0041
GO:0006975	DNA damage induced protein phosphorylation	6	2	0.0043
GO:0032264	IMP salvage	6	2	0.0043
GO:0001774	microglial cell activation	21	3	0.0055
GO:0090399	replicative senescence	7	2	0.006

GO:0050968	detection of chemical stimulus involved in sensory perception of pain	23	3	0.0072
GO:0030091	protein repair	8	2	0.0079
GO:0045957	negative regulation of complement activation, alternative pathway	8	2	0.0079
GO:1900004	negative regulation of serine-type endopeptidase activity	8	2	0.0079
GO:0045959	negative regulation of complement activation, classical pathway	9	2	0.0101
GO:0045589	regulation of regulatory T cell differentiation	10	2	0.0125
GO:0050954	sensory perception of mechanical stimulus	28	3	0.0125
GO:0046777	protein autophosphorylation	53	4	0.0136
GO:0071312	cellular response to alkaloid	31	3	0.0165
GO:0010044	response to aluminum ion	1	1	0.0175
GO:0032962	positive regulation of inositol trisphosphate biosynthetic process	1	1	0.0175
GO:0034696	response to prostaglandin F	1	1	0.0175
GO:0036466	synaptic vesicle recycling via endosome	1	1	0.0175
GO:0046519	sphingoid metabolic process	1	1	0.0175

GO:0051482	positive regulation of cytosolic calcium ion concentration involved in phospholipase C-activating G-protein coupled signaling pathway	1	1	0.0175
GO:0060716	labyrinthine layer blood vessel development	1	1	0.0175
GO:0070584	mitochondrion morphogenesis	1	1	0.0175
GO:0090149	mitochondrial membrane fission	1	1	0.0175
GO:1900244	positive regulation of synaptic vesicle endocytosis	1	1	0.0175
GO:1904579	cellular response to thapsigargin	1	1	0.0175
GO:1905395	response to flavonoid	1	1	0.0175
GO:1990910	response to hypobaric hypoxia	1	1	0.0175
GO:2000302	positive regulation of synaptic vesicle exocytosis	1	1	0.0175
GO:0006002	fructose 6-phosphate metabolic process	12	2	0.0179
GO:0031122	cytoplasmic microtubule organization	12	2	0.0179
GO:0032968	positive regulation of transcription elongation from RNA polymerase II promoter	12	2	0.0179
GO:0015074	DNA integration	33	3	0.0195
GO:0000398	mRNA splicing, via spliceosome	90	5	0.0205

GO:0090307	mitotic spindle assembly	13	2	0.0209
GO:0031098	stress-activated protein kinase signaling cascade	107	3	0.0242
GO:0032507	maintenance of protein location in cell	15	2	0.0274
GO:0043312	neutrophil degranulation	66	4	0.0281
GO:0051289	protein homotetramerization	66	4	0.0281
GO:0007286	spermatid development	16	2	0.031
GO:0007344	pronuclear fusion	2	1	0.0346
GO:0010569	regulation of double-strand break repair via homologous recombination	2	1	0.0346
GO:0010701	positive regulation of norepinephrine secretion	2	1	0.0346
GO:0010767	regulation of transcription from RNA polymerase II promoter in response to UV-induced DNA damage	2	1	0.0346
GO:0016325	oocyte microtubule cytoskeleton organization	2	1	0.0346
GO:0016559	peroxisome fission	2	1	0.0346
GO:0019509	L-methionine salvage from methylthioadenosine	2	1	0.0346
GO:0023016	signal transduction by trans-phosphorylation	2	1	0.0346

GO:0032298	positive regulation of DNA-dependent DNA replication initiation	2	1	0.0346
GO:0034311	diol metabolic process	2	1	0.0346
GO:0036438	maintenance of lens transparency	2	1	0.0346
GO:0045196	establishment or maintenance of neuroblast polarity	2	1	0.0346
GO:0045450	bicoid mRNA localization	2	1	0.0346
GO:0061003	positive regulation of dendritic spine morphogenesis	2	1	0.0346
GO:0071476	cellular hypotonic response	2	1	0.0346
GO:0072425	signal transduction involved in G2 DNA damage checkpoint	2	1	0.0346
GO:0090188	negative regulation of pancreatic juice secretion	2	1	0.0346
GO:0090200	positive regulation of release of cytochrome c from mitochondria	2	1	0.0346
GO:1900063	regulation of peroxisome organization	2	1	0.0346
GO:1905408	negative regulation of creatine transmembrane transporter activity	2	1	0.0346
GO:2000650	negative regulation of sodium ion transmembrane transporter activity	2	1	0.0346
GO:2000681	negative regulation of rubidium ion transport	2	1	0.0346

GO:0051570	regulation of histone H3-K9 methylation	17	2	0.0347
GO:0034605	cellular response to heat	42	3	0.0366
GO:0000289	nuclear-transcribed mRNA poly(A) tail shortening	18	2	0.0387
GO:0071356	cellular response to tumor necrosis factor	126	6	0.0414
GO:0046605	regulation of centrosome cycle	19	2	0.0427
GO:0045429	positive regulation of nitric oxide biosynthetic process	45	3	0.0436
GO:0043434	response to peptide hormone	76	4	0.0437

1133

1134 **Supplementary Table 2.** Gene ontology enrichment analysis results comparing the
1135 transcriptional profiles of *D. trenchii* when *in hospite* at 28 °C to the free-living stage at
1136 28 °C

GO ID	Term	Annotated	Significant	FDR
GO:0003341	cilium movement	36	13	5.10E-11
GO:0001539	cilium or flagellum-dependent cell motility	27	9	1.20E-07
GO:0009250	glucan biosynthetic process	61	10	0.00012
GO:1904146	positive regulation of meiotic cell cycle process involved in oocyte maturation	4	3	0.00014
GO:0007089	traversing start control point of mitotic cell cycle	2	2	0.00109
GO:0015671	oxygen transport	25	5	0.00117
GO:0015701	bicarbonate transport	26	5	0.00141
GO:0045957	negative regulation of complement activation, alternative pathway	8	3	0.00177
GO:1900004	negative regulation of serine-type endopeptidase activity	8	3	0.00177
GO:0045959	negative regulation of complement activation, classical pathway	9	3	0.00258
GO:0045589	regulation of regulatory T cell differentiation	10	3	0.0036
GO:0042744	hydrogen peroxide catabolic process	32	5	0.00368
GO:0006865	amino acid transport	123	12	0.00569

GO:0007157	heterophilic cell-cell adhesion via plasma membrane cell adhesion molecules	12	3	0.00629
GO:0051965	positive regulation of synapse assembly	13	3	0.00797
GO:0070317	negative regulation of G0 to G1 transition	5	2	0.01017
GO:0045454	cell redox homeostasis	134	10	0.01322
GO:0003374	dynamin family protein polymerization in mitochondrial fission	6	2	0.01493
GO:0006452	translational frameshifting	6	2	0.01493
GO:1902475	L-alpha-amino acid transmembrane transport	6	2	0.01493
GO:0050775	positive regulation of dendrite morphogenesis	7	2	0.02045
GO:0006813	potassium ion transport	115	8	0.02218
GO:0030091	protein repair	8	2	0.02668
GO:0098869	cellular oxidant detoxification	53	5	0.02997
GO:0010044	response to aluminum ion	1	1	0.03302
GO:0032962	positive regulation of inositol trisphosphate biosynthetic process	1	1	0.03302
GO:0034696	response to prostaglandin F	1	1	0.03302

GO:0035444	nickel cation transmembrane transport	1	1	0.03302
GO:0036466	synaptic vesicle recycling via endosome	1	1	0.03302
GO:0042908	xenobiotic transport	1	1	0.03302
GO:0051482	positive regulation of cytosolic calcium ion concentration involved in phospholipase C-activating G-protein coupled signaling pathway	1	1	0.03302
GO:0060716	labyrinthine layer blood vessel development	1	1	0.03302
GO:0070407	oxidation-dependent protein catabolic process	1	1	0.03302
GO:0070584	mitochondrion morphogenesis	1	1	0.03302
GO:0072432	response to G1 DNA damage checkpoint signaling	1	1	0.03302
GO:0090149	mitochondrial membrane fission	1	1	0.03302
GO:0090296	regulation of mitochondrial DNA replication	1	1	0.03302
GO:1900244	positive regulation of synaptic vesicle endocytosis	1	1	0.03302
GO:1904579	cellular response to thapsigargin	1	1	0.03302
GO:1905395	response to flavonoid	1	1	0.03302

GO:1990910	response to hypobaric hypoxia	1	1	0.03302
GO:2000302	positive regulation of synaptic vesicle exocytosis	1	1	0.03302
GO:0006898	receptor-mediated endocytosis	104	8	0.03359
GO:0051291	protein heterooligomerization	55	5	0.03447
GO:0000289	nuclear-transcribed mRNA poly(A) tail shortening	18	3	0.0489

1137

1138 **Supplementary Table 3.** Gene ontology enrichment analysis results comparing the

1139 transcriptional profiles of *D. trenchii* when *in hospite* at 34 °C to the free-living stage at

1140 34 °C.

1141

GO ID	Term	Annotated	Significant	FDR
GO:0042545	cell wall modification	2	1	0.01
GO:0007218	neuropeptide signaling pathway	3	1	0.015
GO:0019594	mannitol metabolic process	3	1	0.015
GO:0060012	synaptic transmission, glycinergic	3	1	0.015
GO:0070247	regulation of natural killer cell apoptotic process	3	1	0.015
GO:0071266	de novo' L-methionine biosynthetic process	3	1	0.015
GO:1990001	inhibition of cysteine-type endopeptidase activity involved in apoptotic process	4	1	0.02
GO:0007023	post-chaperonin tubulin folding pathway	5	1	0.025
GO:0015801	aromatic amino acid transport	5	1	0.025
GO:0045899	positive regulation of RNA polymerase II transcriptional preinitation complex assembly	6	1	0.03
GO:0000186	activation of MAPKK activity	7	1	0.034
GO:0032801	receptor catabolic process	8	1	0.039
GO:0045957	negative regulation of complement activation, alternative pathway	8	1	0.039

GO:1900004	negative regulation of serine-type endopeptidase activity	8	1	0.039
GO:0045959	negative regulation of complement activation, classical pathway	9	1	0.044
GO:0006072	glycerol-3-phosphate metabolic process	10	1	0.049
GO:0045589	regulation of regulatory T cell differentiation	10	1	0.049
GO:0060056	mammary gland involution	10	1	0.049

1142

1143 **Supplementary Table 4.** Gene ontology enrichment analysis results comparing the

1144 transcriptional profiles of *D. trenchii* when free-living at 34 °C to the free-living stage at

1145 28 °C.

1146

GO ID	Term	Annotated	Significant	FDR
GO:0010021	amylopectin biosynthetic process	2	1	0.014
GO:0045454	cell redox homeostasis	134	4	0.015
GO:0005978	glycogen biosynthetic process	30	2	0.019
GO:0007523	larval visceral muscle development	3	1	0.021
GO:0036059	nephrocyte diaphragm assembly	3	1	0.021
GO:0046832	negative regulation of RNA export from nucleus	3	1	0.021
GO:0071108	protein K48-linked deubiquitination	3	1	0.021
GO:0007156	homophilic cell adhesion via plasma membrane adhesion molecules	4	1	0.028
GO:0070536	protein K63-linked deubiquitination	4	1	0.028
GO:0097206	nephrocyte filtration	5	1	0.035

GO:0006426	glycyl-tRNA aminoacylation	6	1	0.042
GO:0042128	nitrate assimilation	6	1	0.042
GO:0045899	positive regulation of RNA polymerase II transcriptional preinitiation complex assembly	6	1	0.042
GO:0051292	nuclear pore complex assembly	6	1	0.042
GO:0006474	N-terminal protein amino acid acetylation	7	1	0.049
GO:0006542	glutamine biosynthetic process	7	1	0.049
GO:0007076	mitotic chromosome condensation	7	1	0.049

1147

1148 **Supplementary Table 5.** Gene ontology enrichment analysis results comparing the

1149 transcriptional profiles of *D. trenchii* when *in hospite* at 34 °C to symbiosis at 28 °C.

1150

1151

1152

1153

1154

1155